The Structure of the

$\gamma =$ 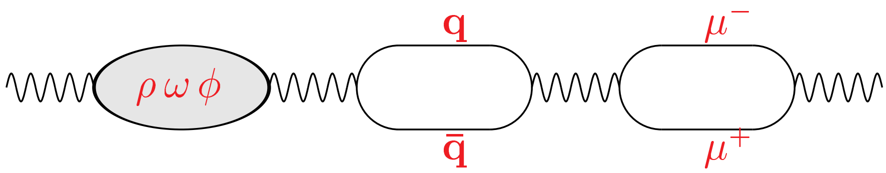

Richard Nisius (CERN)

25.05.01

- Introduction

1) Electron-Photon DIS
   - a) QED Structure
   - b) Hadronic Structure

2) Results from Other Reactions
   - a) Photon-Photon Scattering
   - b) Results from HERA

- Conclusions

For more Information please consult:
http://home.cern.ch/nisius, and
R. Nisius, Phys.Rep. 332 (2000) 165, (hep-ex/9912049).

The ’history’ of the Photon

Date	Event
8.11.1895	Röntgen discovers the X-rays (first Nobel Prize for physics 1901).
1900	Planck interprets light as ’energy quanta’ $E = h\,\nu$, with $h = 6.626 \cdot 10^{-34} Js$.
1905	Einstein explains the photoelectric effect by ’photons’.
1922	Discovery of Compton scattering $\mathrm{e}\gamma \longrightarrow \mathrm{e}'\gamma'$.
1927	Heisenberg formulates the uncertainty principle e. g. $\Delta E \Delta t \geq \hbar$.
1930	Fist attempt to measure photon-photon scattering by Hughes et. al.
1936	First calculation of photon-photon scattering by Euler und Kockel.
1981	First measurement of the hadronic structure function of the photon by PLUTO.
2011	The Higgs Boson will be produced through photon-photon fusion at TESLA?

Properties of the photon

Property	
Mass (m)	$0 \quad (m/m_{\rm e} < 4 \cdot 10^{-22},$ [1])
Charge (Q)	$0 \quad (Q/Q_{\rm e} < 5 \cdot 10^{-30},$ [2])
Velocity (c)	299792458 m/s
Spin parity ($\rm J^{PC}$)	1^{--}
Coupling (α)	$1/137.03599976(50)$
Task	Carrier of the electromagnetic interaction, no self-coupling

[1] Roderic Lakes, Phys. Rev. Lett. 80 (1998) 1826.

[2] Georg Raffelt, Phys. Rev. D50 (1994) 7792.

Charge determination

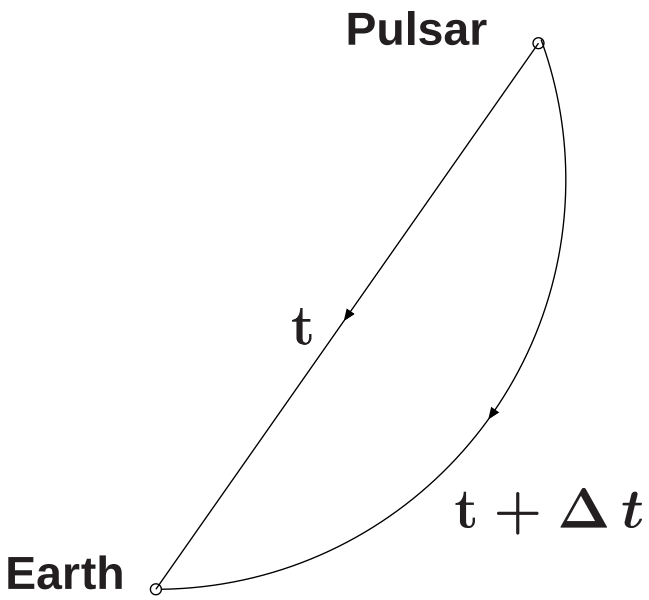

1. Pulsars are very distant sources of photons.
2. If photons carry charge they are subject to the Lorentz force and their trajectories in a magnetic field are bend.
3. This results in an energy dependent variation of the travel time of $\frac{\Delta t}{t} = \frac{Q^2 B^2 l^2}{6E^2}$.
4. Using the observed dispersion of the photon pulses from the pulsar PSR 1937+21 an upper limit for the charge of $Q/Q_\mathrm{e} < 5 \cdot 10^{-30}$ is deduced.

---

[2] Georg Raffelt, Phys. Rev. D50 (1994) 7792.

Photon-photon scattering anno 1930

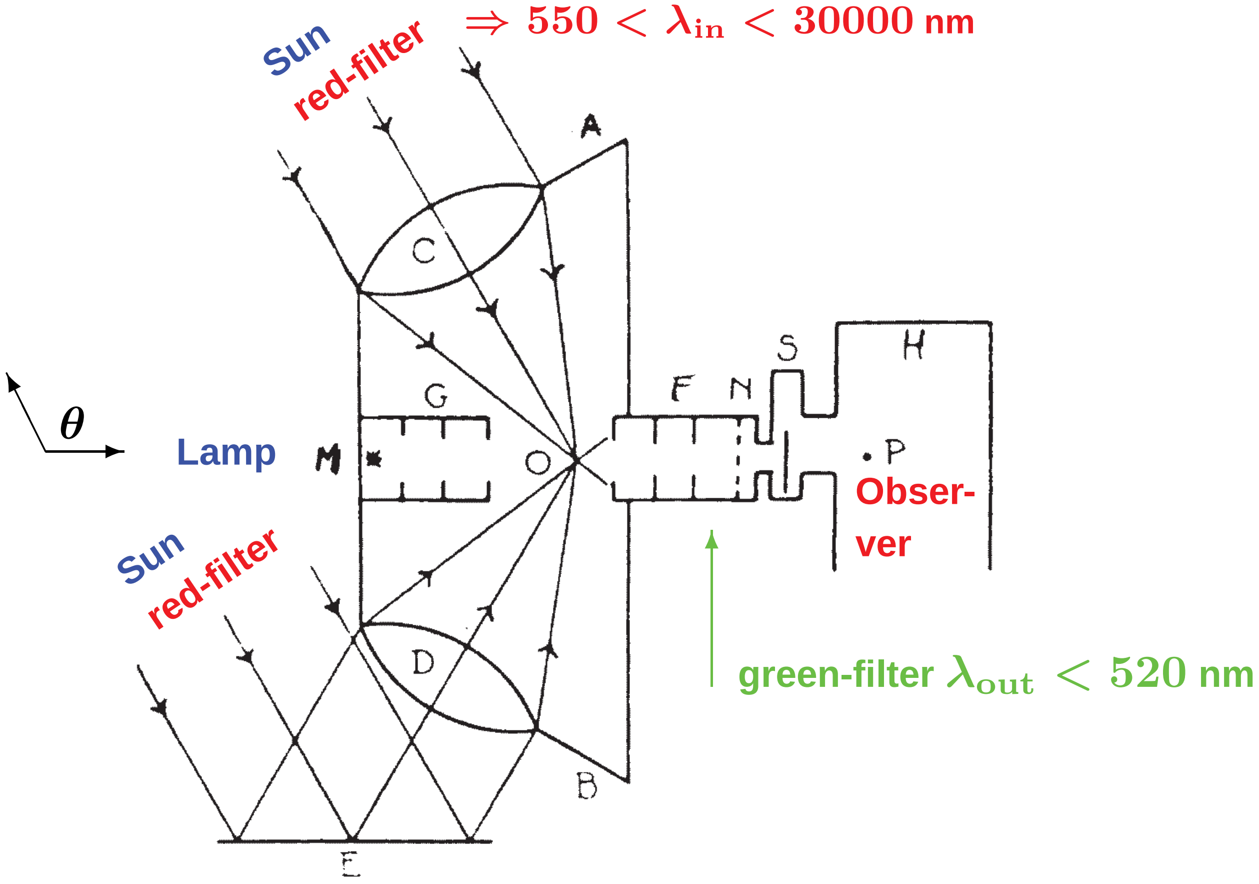

Fig. 2. Diagram of apparatus.

$$\gamma_1(\lambda_{in})\gamma_2(\lambda_{in}) \rightarrow \gamma_1'(\lambda_{out})\gamma_2'(\lambda_{out})$$

with: $$\lambda_{out} = \lambda_{in}(1+\cos\theta)$$

No light was observed.

$$\Rightarrow \sigma_{\gamma\gamma\rightarrow\gamma\gamma} < 3\cdot 10^8 \text{ pb}$$

A.L. Hughes and G.E.M. Jauncey, Phys.Rev. 36 (1930) 773.

Cross-section for photon-photon scattering

For low energy photons with $E_\gamma = h\nu \ll m_\mathrm{e}c^2$ follows:

$$\frac{\sigma_{\gamma\gamma\to\gamma\gamma}}{d\Omega} = \frac{139}{32400\pi}\alpha^2 r_\mathrm{e}^2 \left(\frac{h\nu}{m_\mathrm{e}c^2}\right)^6 \left(3+\cos^2\theta\right)^2$$

$$\frac{\sigma_{\gamma\gamma\to\gamma\gamma}}{\mathrm{pb}} = 0.73\cdot 10^{-29}\cdot\left(\frac{h\nu}{\mathrm{eV}}\right)^6$$

For visible light, $\lambda = 400 - 700$ nm, one gets:

$$\boxed{\sigma_{\gamma\gamma\to\gamma\gamma} = (2.2-64)\cdot 10^{-28}\ \text{pb}}$$

H. Euler and B. Kockel, Ann. der Phys. 26 (1936) 398.

Photon-photon scattering anno 1996

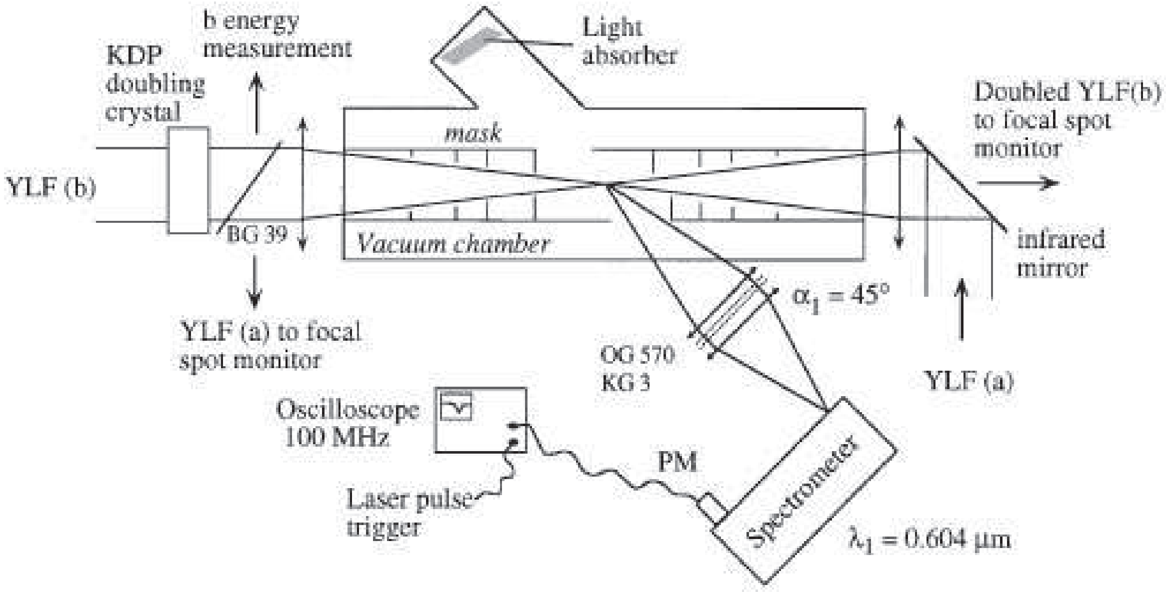

Fig. 2. Schematics of the experimental set-up. Two synchronized laser beams at $\lambda_0 = 1.053$ μm and $\lambda_0/2$ are focussed to a common focal spot. A photon-photon collision can give a scattered photon detected at $\alpha_1 = 45°$ with $\lambda_1 = 0.604$ μm wavelength. We did not attempt to observe the other scattered photon at $\alpha_2 = 79°$ with $\lambda_2 = 0.838$ μm

The sensitivity was much improved by using mono-chromatic, high-intensity laser and the possibility to detect single photons.

No signal has been observed.

$$\Rightarrow \sigma_{\gamma\gamma\to\gamma\gamma} < 9.9 \cdot 10^{-4} \text{ pb}$$

F. Moulin et. al, Z.Phys. C72 (1996) 607.

The photon in our world

Observation	photon energy
	meV
Rotations of molecules	
	eV
Spectrum of the sun	
Hydrogen atomic spectra	
	keV
X-ray radiation	
	MeV
e^+e^- pair creation	
	GeV
$\Rightarrow$ Bremsstrahlung at LEP	$\Leftarrow$
	TeV
Cosmic rays	

The photon in the standard model

The building blocs of matter

Quarks $\begin{pmatrix} u \\ d \end{pmatrix} \begin{pmatrix} c \\ s \end{pmatrix} \begin{pmatrix} t \\ b \end{pmatrix}$

Leptons $\begin{pmatrix} \nu_{\mathrm{e}} \\ \mathrm{e} \end{pmatrix} \begin{pmatrix} \nu_{\mu} \\ \mu \end{pmatrix} \begin{pmatrix} \nu_{\tau} \\ \tau \end{pmatrix}$

Interactions of matter via gauge bosons

Photon (γ), $W^{\pm}$ and Z^{0} bosons and gluons

Gauge boson measurements at LEP

Object	Measurement
Z^0	Precision measurements at LEP100
$W^{\pm}$	M_W to $40\ \mathrm{MeV}$ by LEP200
Gluons	QCD coupling α_s (M_{Z^0}) to about 5% at LEP100
Photon	Photon structure to 10—30% at LEP100—200

Measurements of the photon structure give insight into a fundamental gauge boson of the standard model.

Why do we talk about Photon Structure?

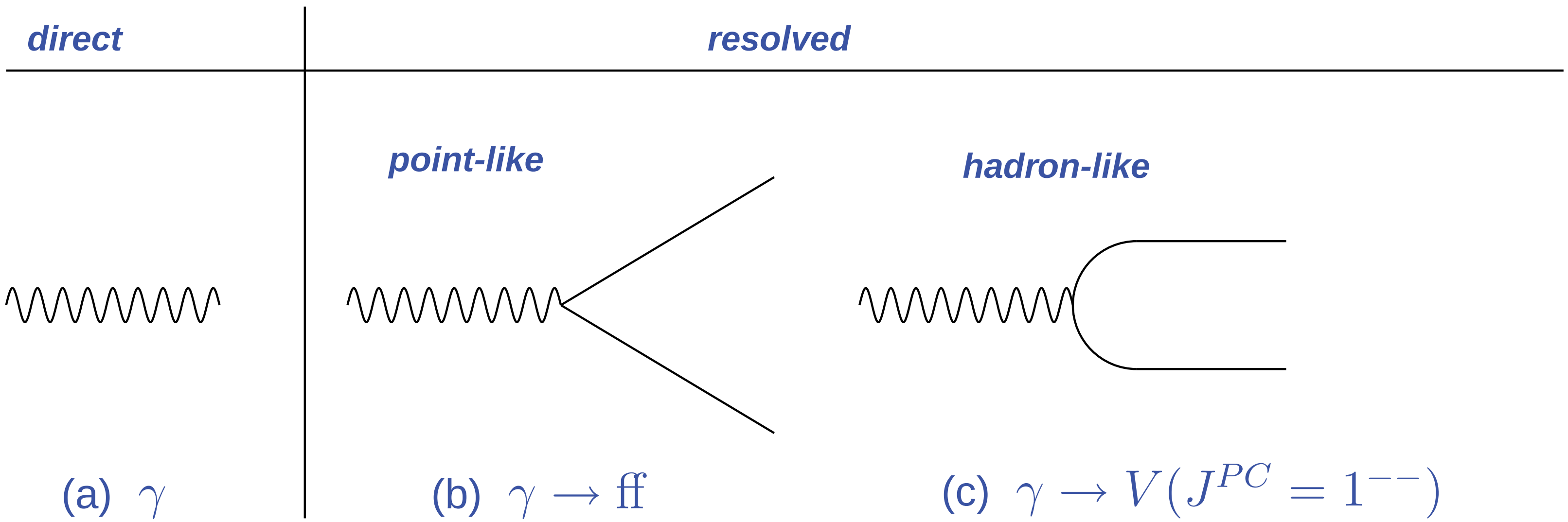

In (a) the whole photon interacts $\Rightarrow$ NO structure

The fluctuations (b,c) exist due to the uncertainty principle $\Rightarrow$ Photon 'Structure'

The typical lifetime of the fluctuations increases with the photon energy and decreases with the photon virtuality

Predictions for the photon structure

QED structure

1. The point-like component leads to a rise of the QED structure at large x.
2. The structure of virtual photons is suppressed.
3. Virtual photons have a longitudinal component.
4. Interference terms are important for virtual photons.

Hadronic structure

1. The global predictions of QED should work in the region where the point-like component dominates, apart from QCD corrections.
2. The evolution of the photon structure exhibits a positive slope for all values of x.
3. The QCD dynamics enforces a steep rise of the photon structure for small values of x, at fixed Q^2.

The LEP Accelerator

Electron-photon scattering

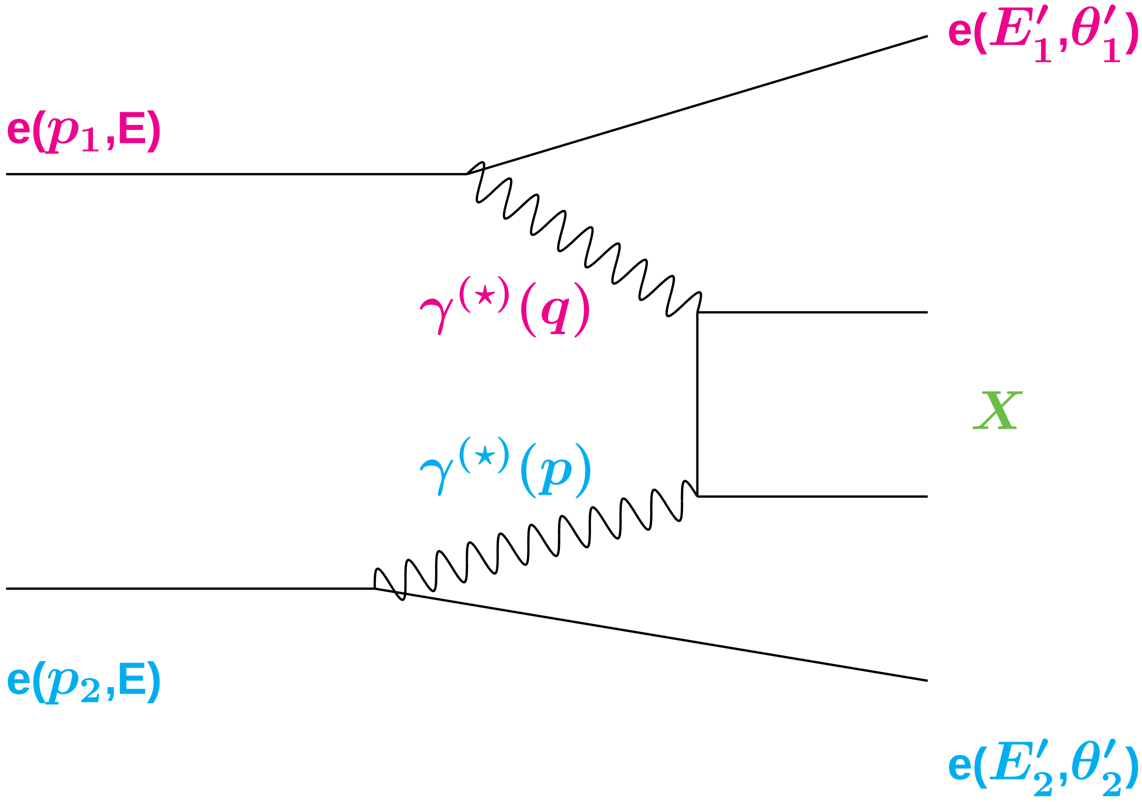

$$\frac{d^4\sigma}{dx\,dQ^2\,dz\,dP^2} \propto \frac{d^2N_\gamma^T}{dz\,dP^2} \cdot \frac{2\pi\alpha^2}{x\,Q^4} \cdot f_y \cdot F_2^\gamma(x, Q^2)$$

with:

$$P^2 = -p^2 = 2\,E\,E'_2\,(1 - \cos\theta'_2)$$

$$\frac{d^2N_\gamma^T}{dz\,dP^2} = \frac{\alpha}{2\pi}\left[\frac{1+(1-z)^2}{z}\frac{1}{P^2} - \frac{2\,m_e^2\,z}{P^4}\right]$$

$$f_y = 1 + (1-y)^2$$

$$Q^2 = -q^2 = 2\,E\,E'_1\,(1 - \cos\theta'_1)$$

$$x = \frac{Q^2}{Q^2 + W^2 + P^2}$$

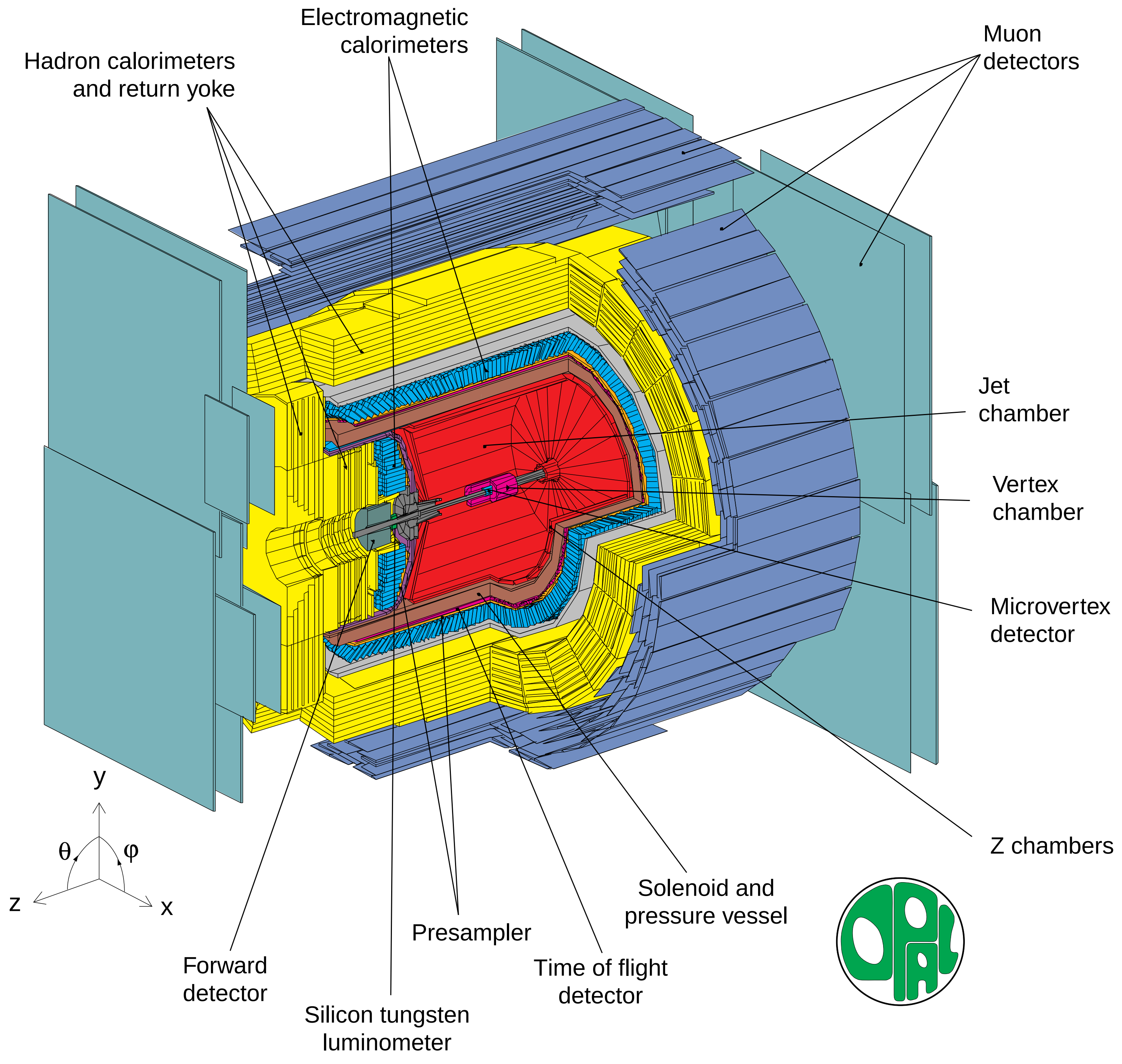
Electromagnetic calorimeters
Hadron calorimeters and return yoke
Muon detectors
Jet chamber
Vertex chamber
Microvertex detector
Z chambers
Solenoid and pressure vessel
Time of flight detector
Presampler
Silicon tungsten luminometer
Forward detector
y
θ
φ
z
x

The muon pair final state

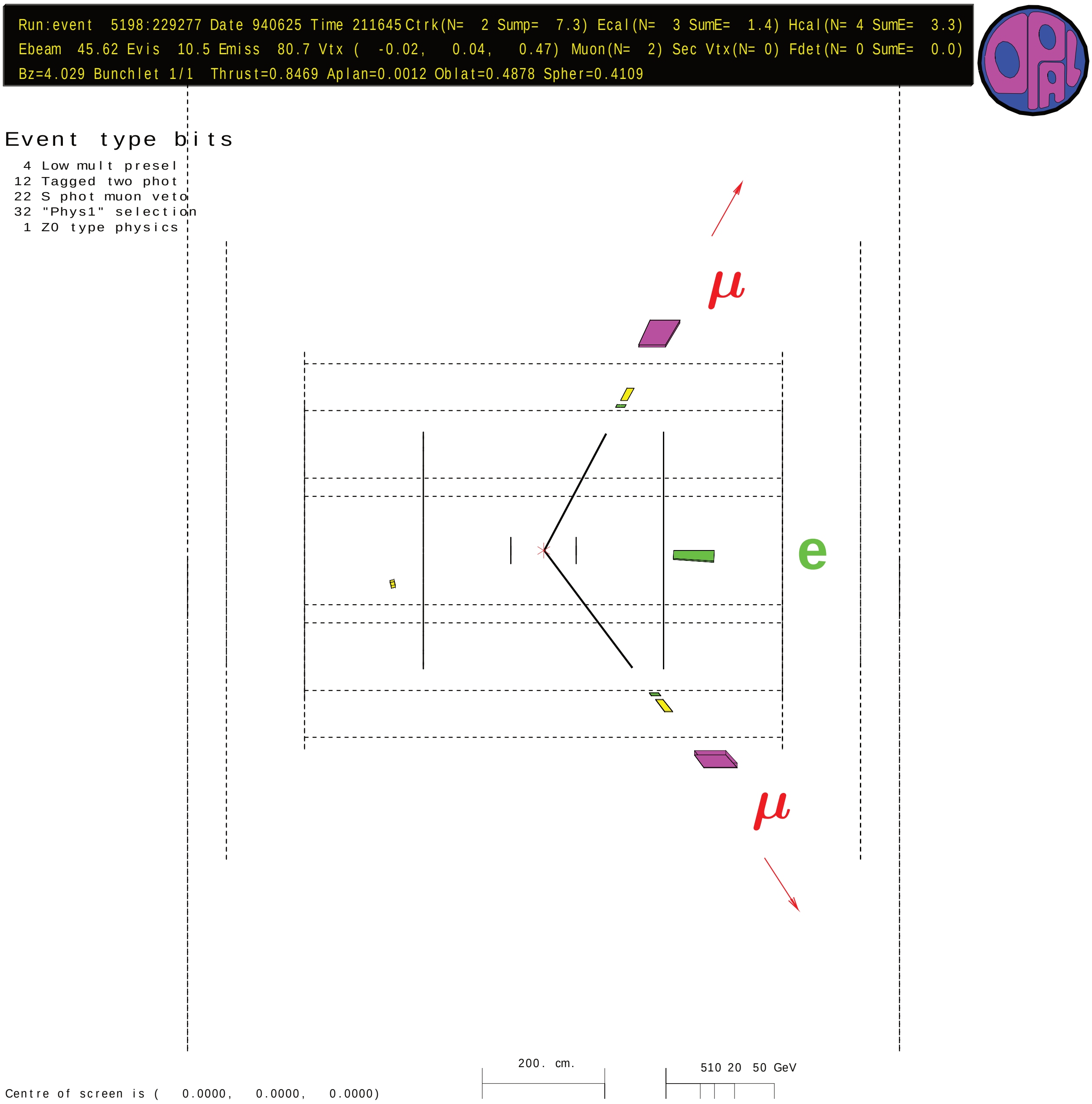

The muon pair final state is a clear topology with good mass resolution.

The world data on $F_{2,\mathrm{QED}}^{\gamma}$

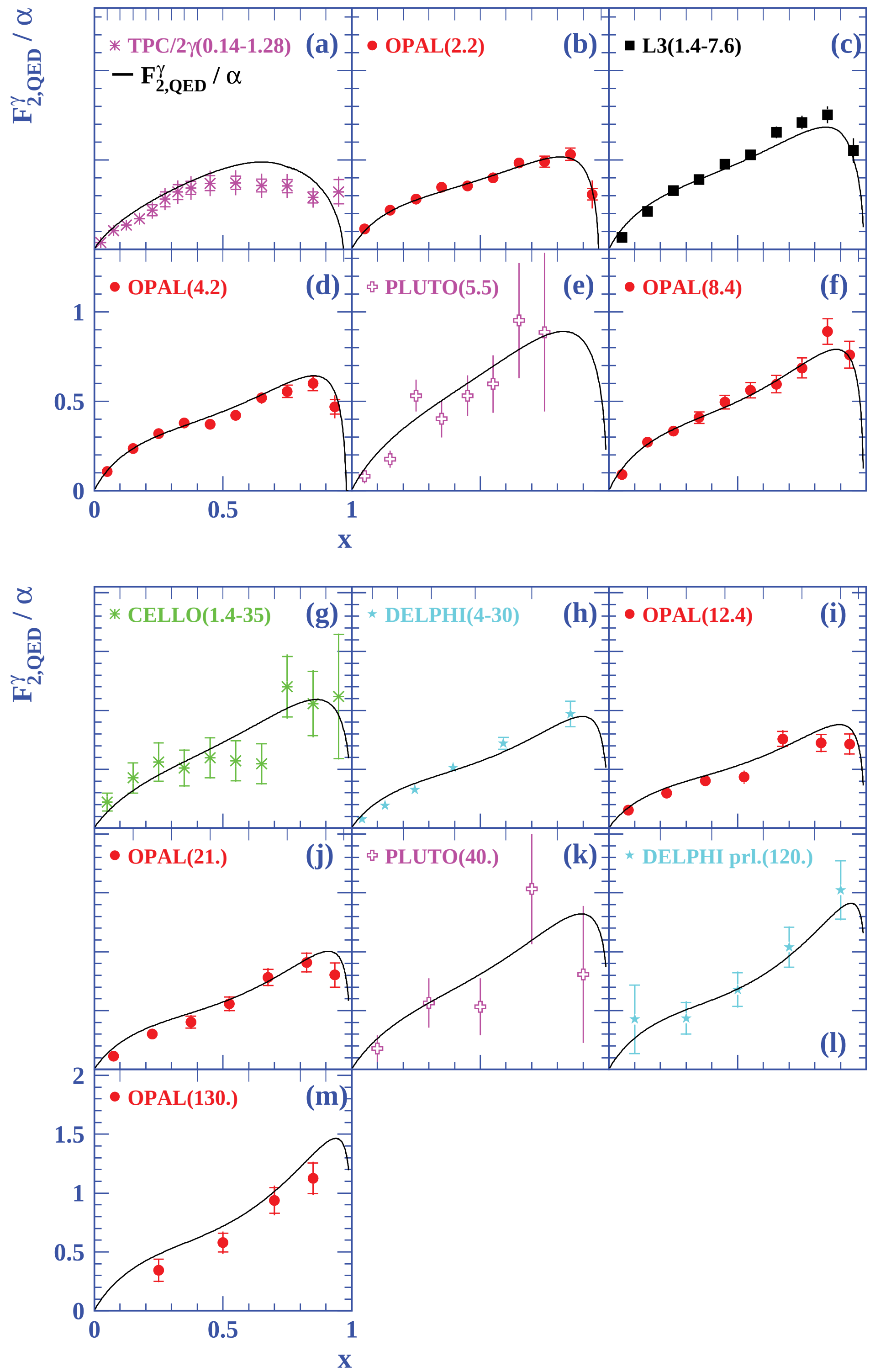

The dependence of $F_{2,\mathrm{QED}}^{\gamma}$ on P^2 and m_μ

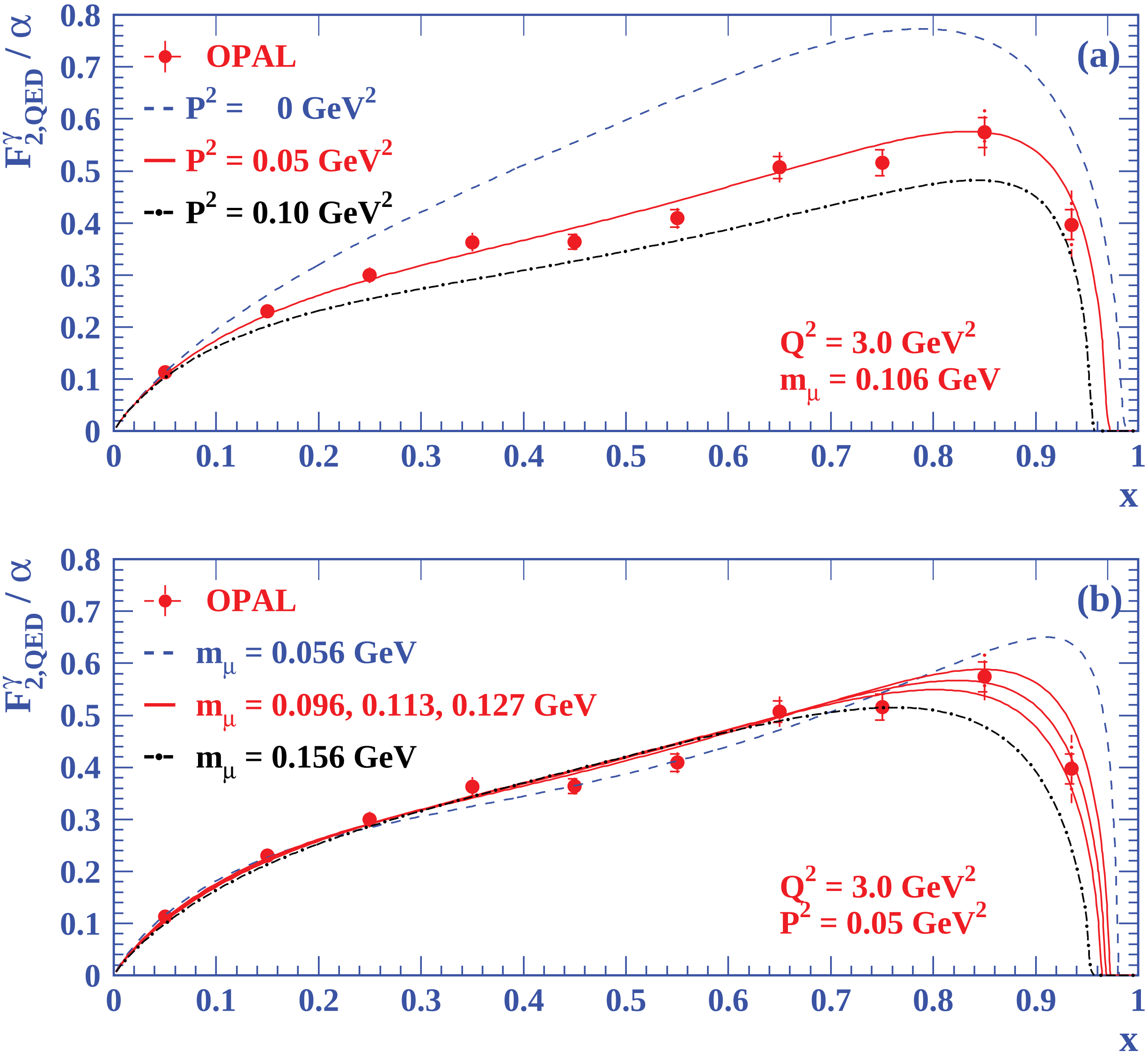

The P^2 dependence is clearly observed in the data.
The muon mass can be determined to about $\pm$15%.

The hadronic final state

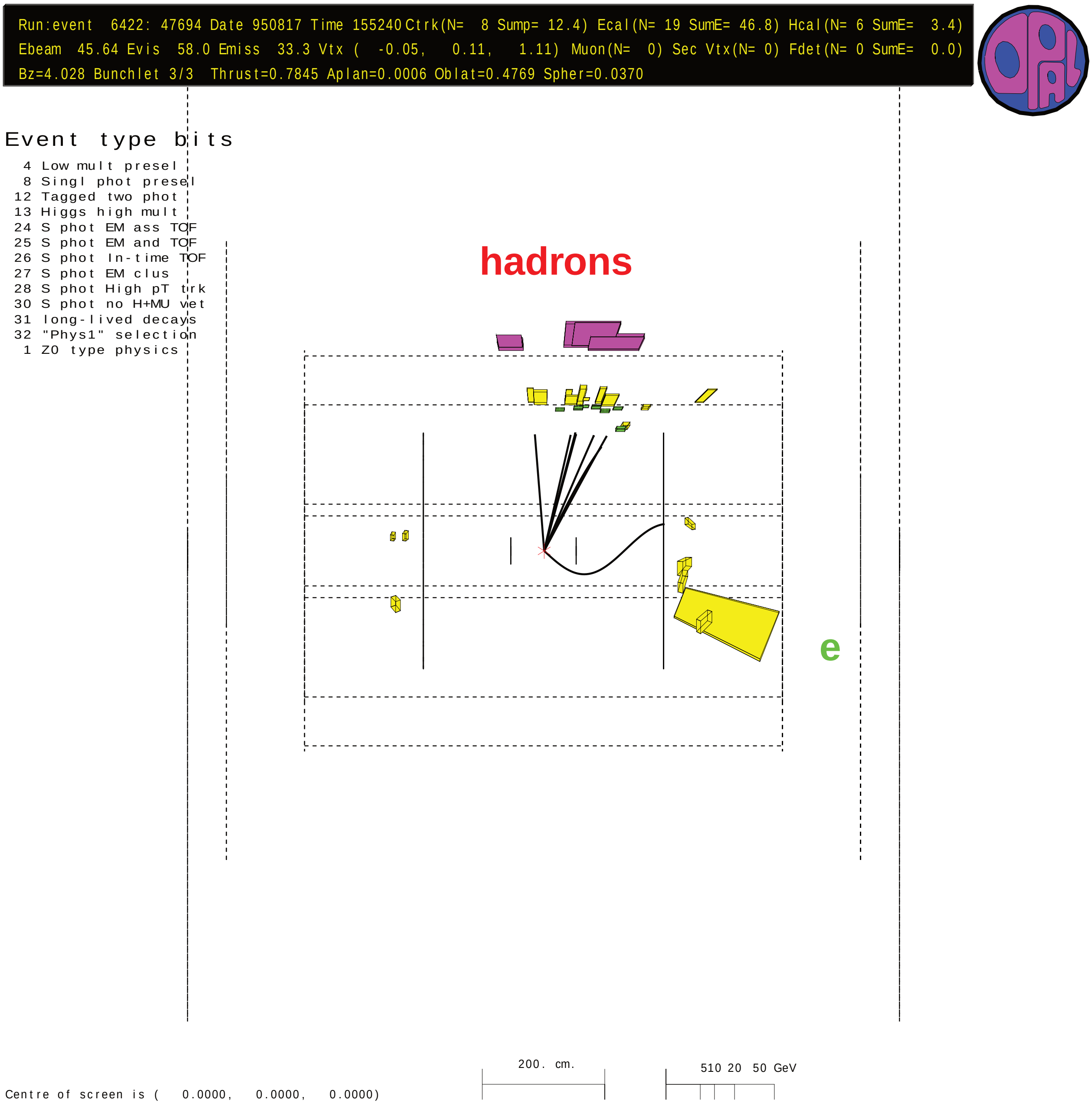

The scattered electron is clearly visible.
However, the hadronic final state may partly disappear along the beam axis.

The description of the hadronic final state

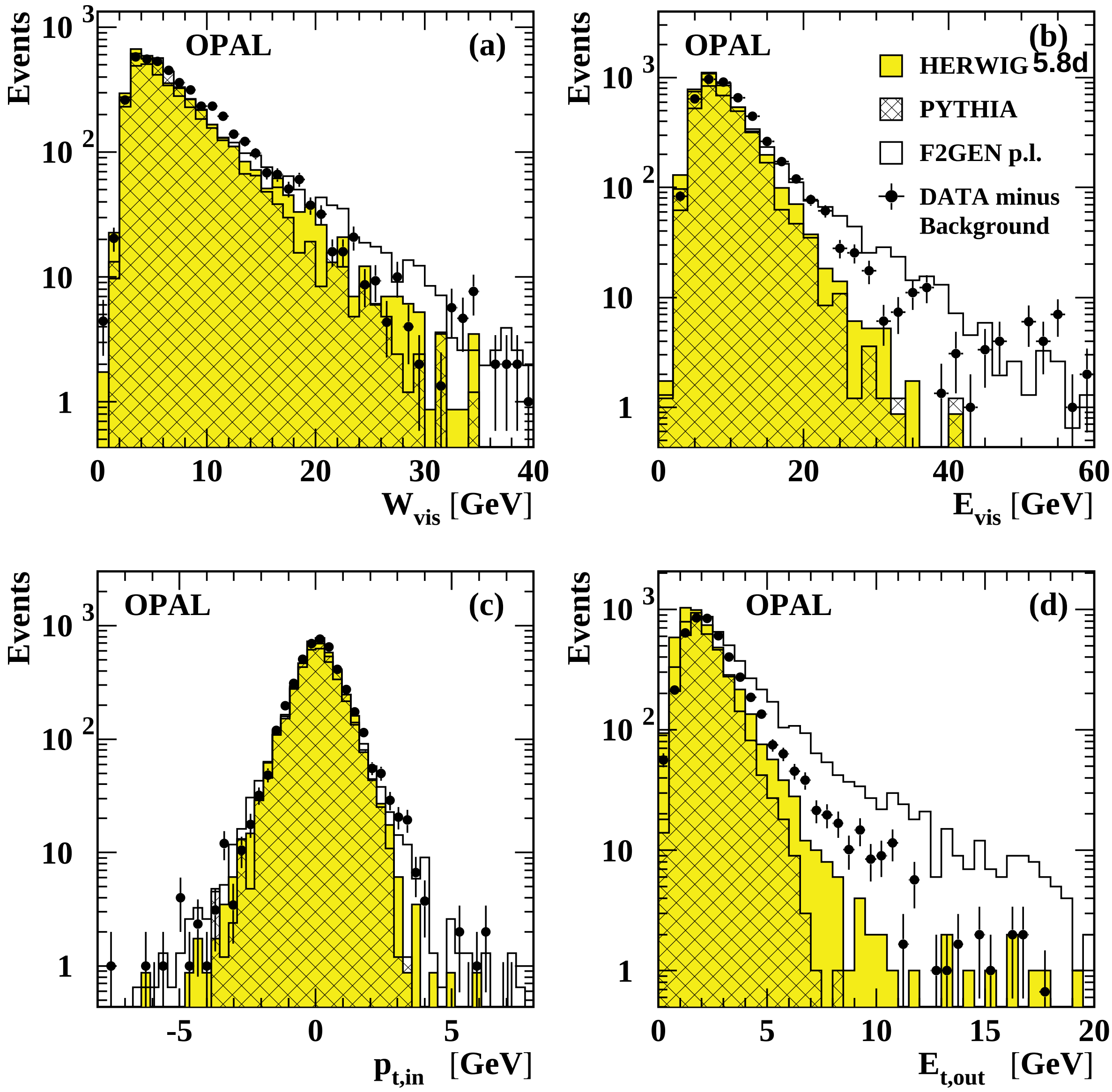

There are significant differences between the data and the Monte Carlo predictions (OPAL ’96)

Comparison to LEP combined data

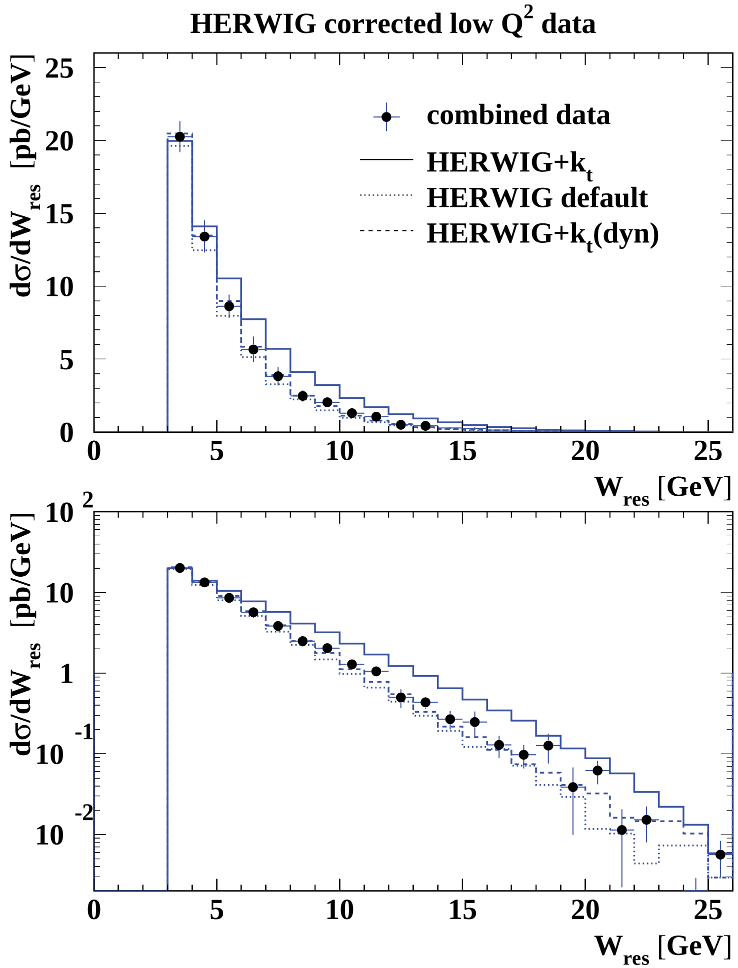

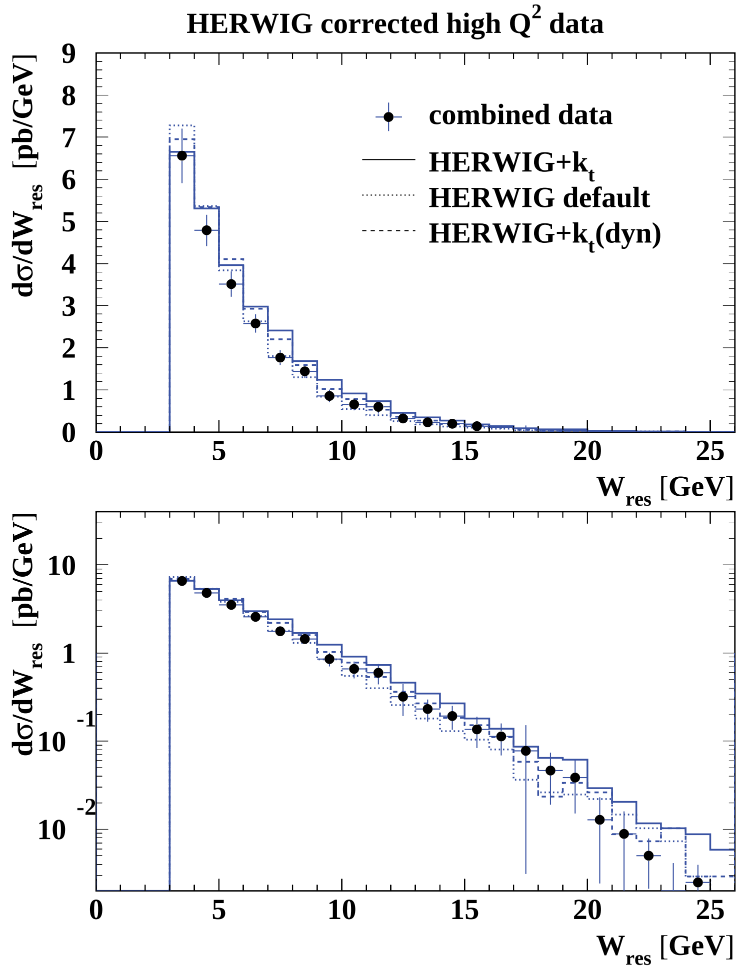

The combined data are a valuable input to constrain the Monte Carlo models (LEP Two-Photon WG CERN-EP-2000-109)

The contributions to $F_2^\gamma(x, Q^2)$

$$F_2^\gamma(x, Q^2) = x \sum_{c,f} e_q^2 \, f_{q,\gamma}(x, Q^2)$$

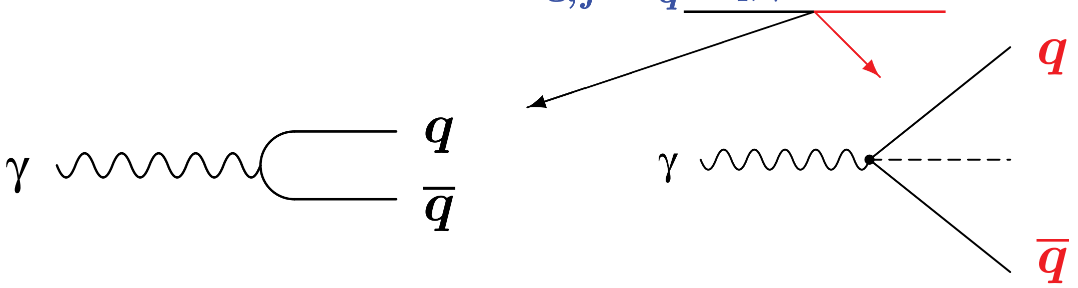

hadron-like, *non–perturbative*

e.g. VMD(ρ, ω, ϕ), low-x

point-like, *perturbative*

high-x

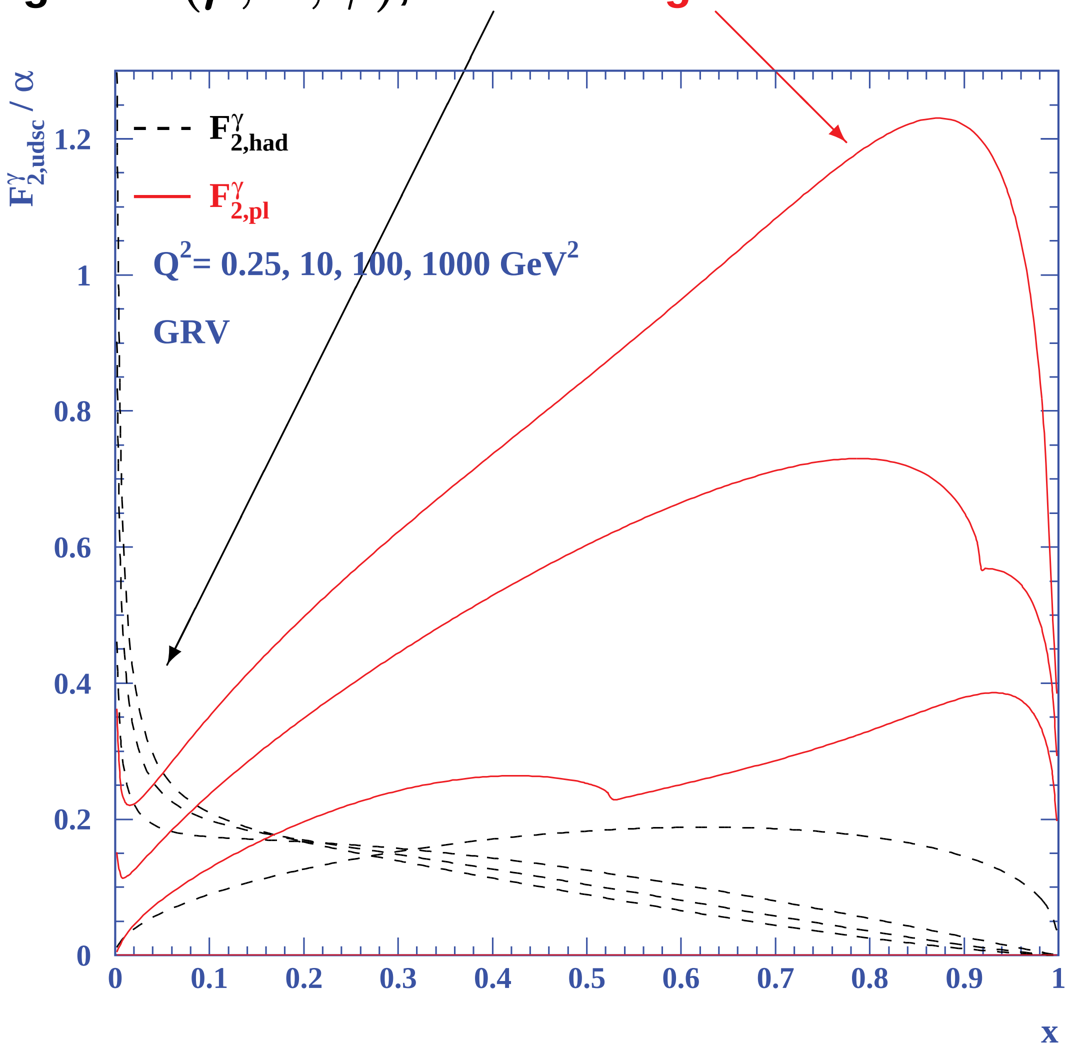

The world data on F_2^γ

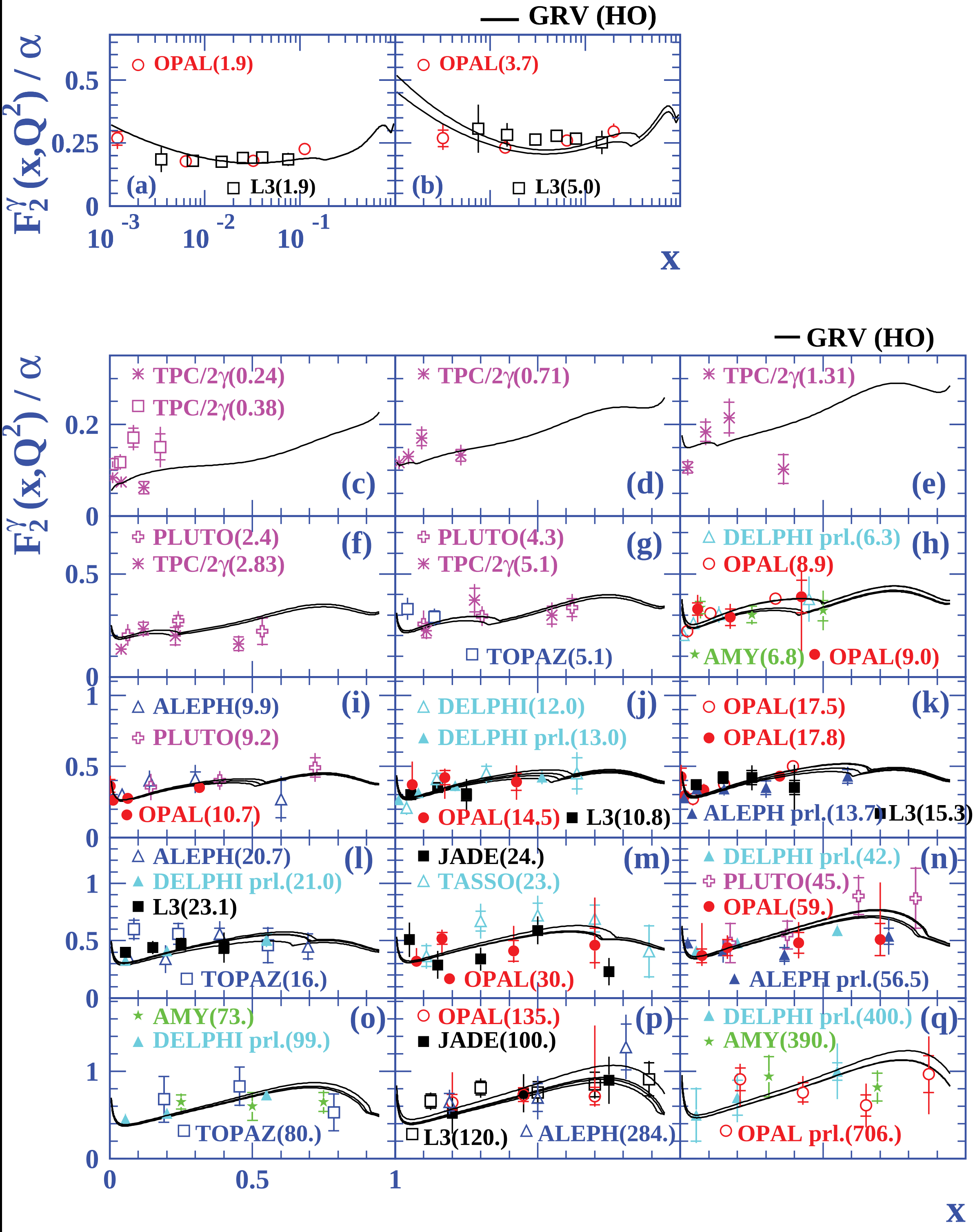

Charm production tagged by D*s

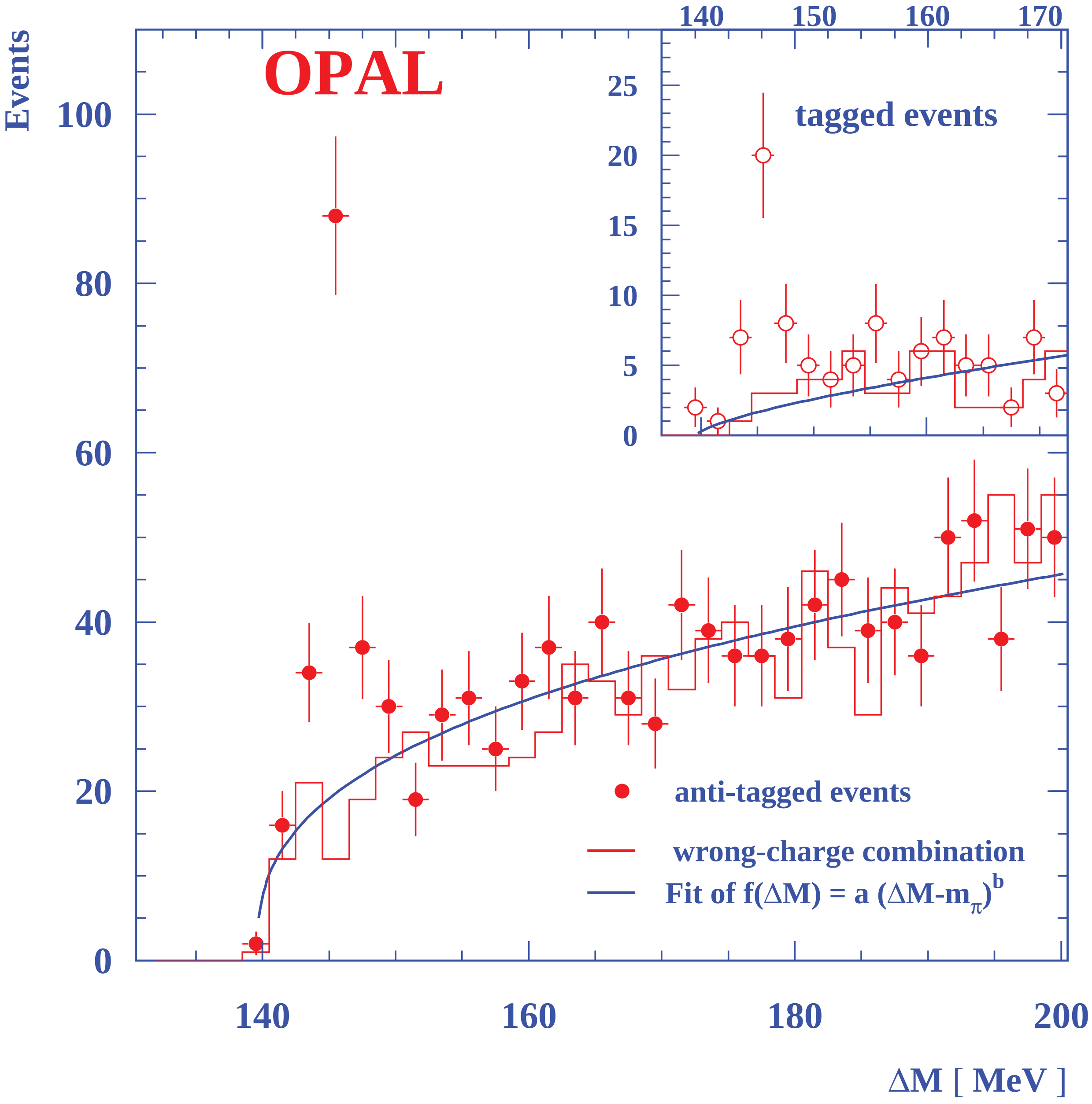

A clear signal in the $\Delta(M) = M(D^\star) - M(D^0)$ mass spectrum is seen for anti-tagged and tagged events

The first measurement of $F_{2,c}^{\gamma}$

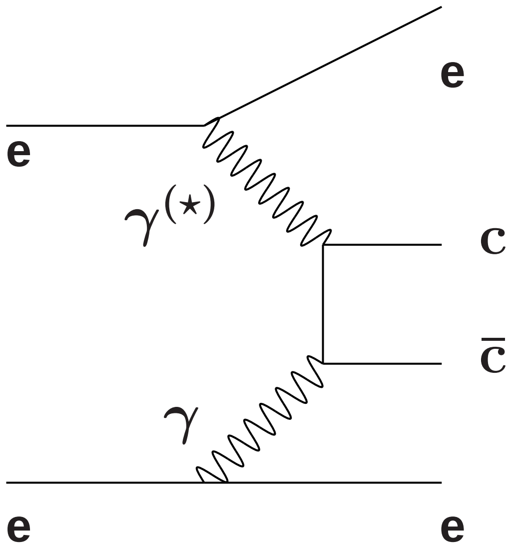

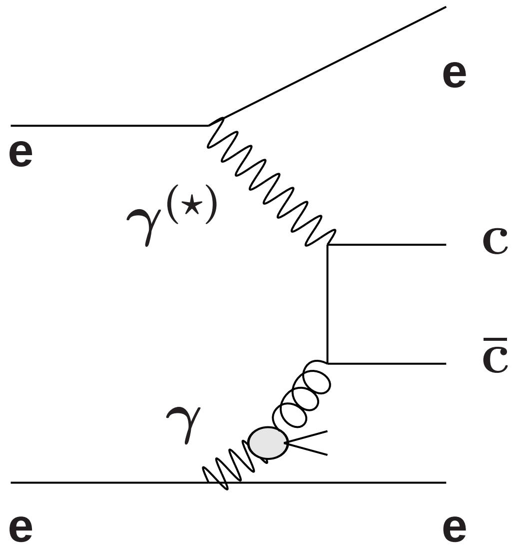

point-like, purely perturbative QCD prediction, dominates at **high-x**

hadron-like, depends on f_g^{γ}, dominates at **low-x**

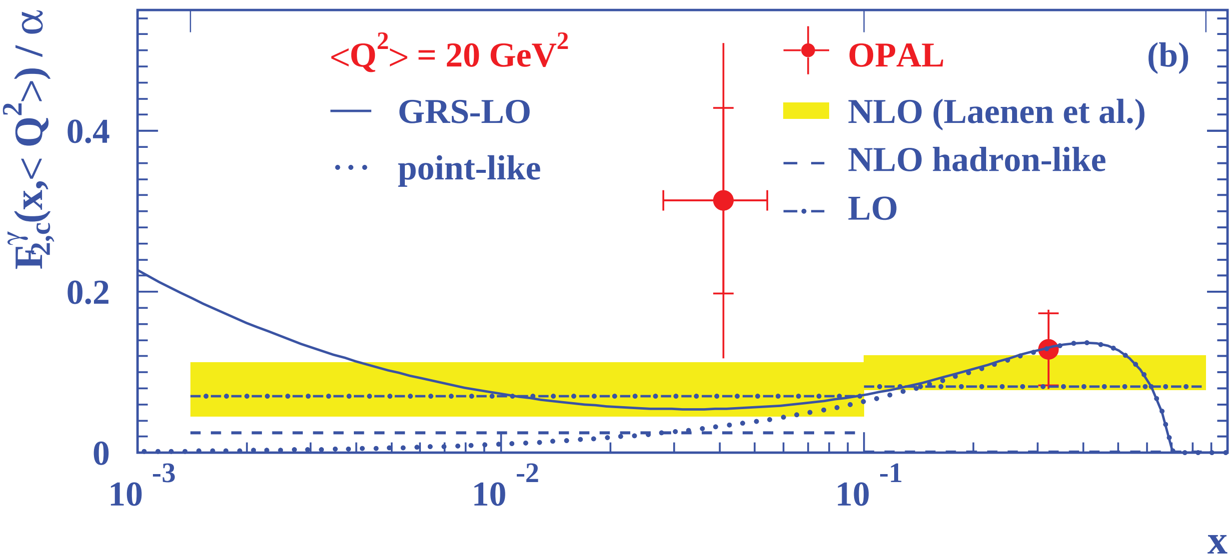

Measurements at low Q^2 and x

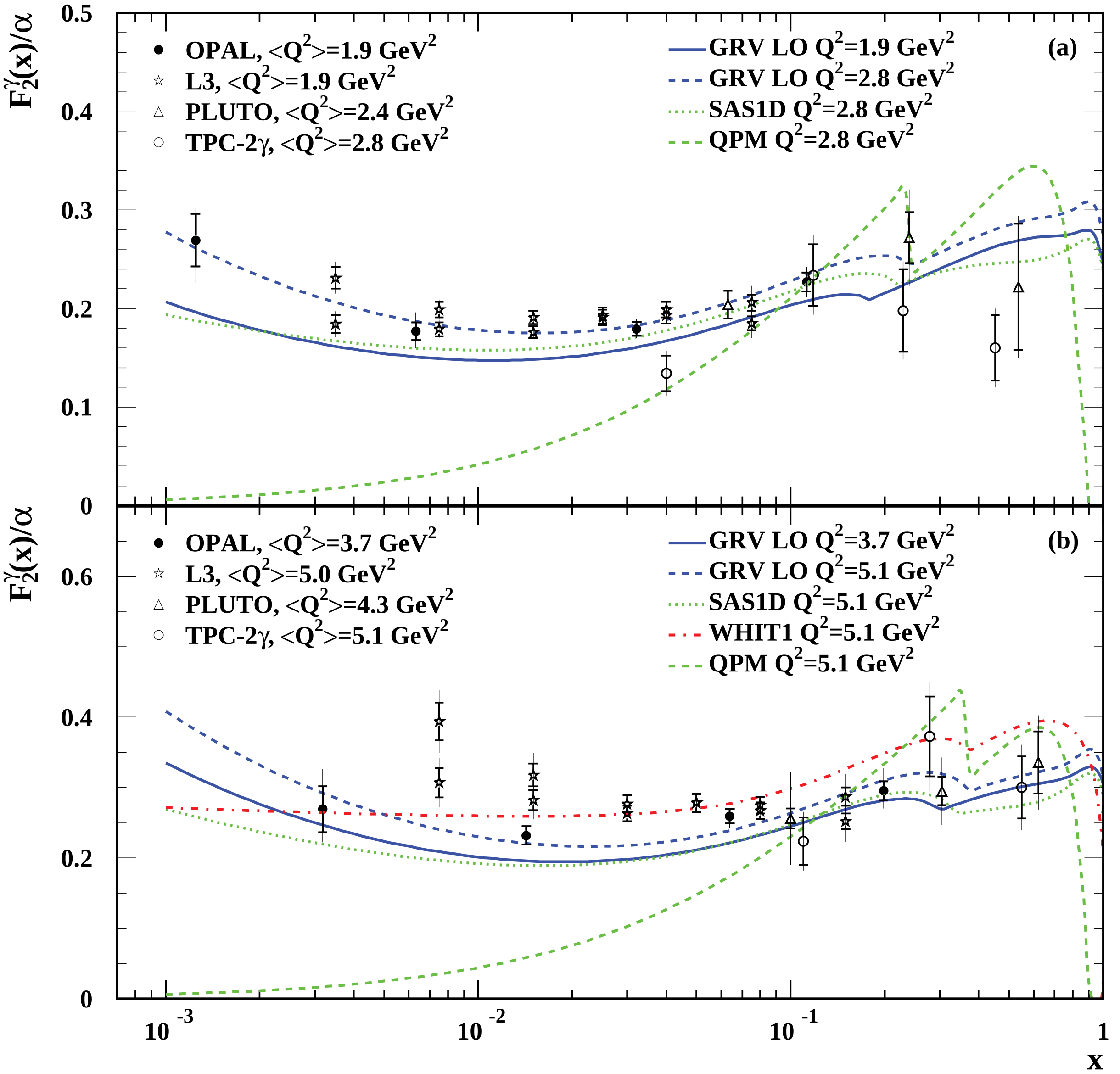

GRV(LO) and SaS1D are slightly too low compared to the data.

OPAL Collab., Eur. Phys. J. C18 (2000) 15.

Q^2 evolution compared to linear fits

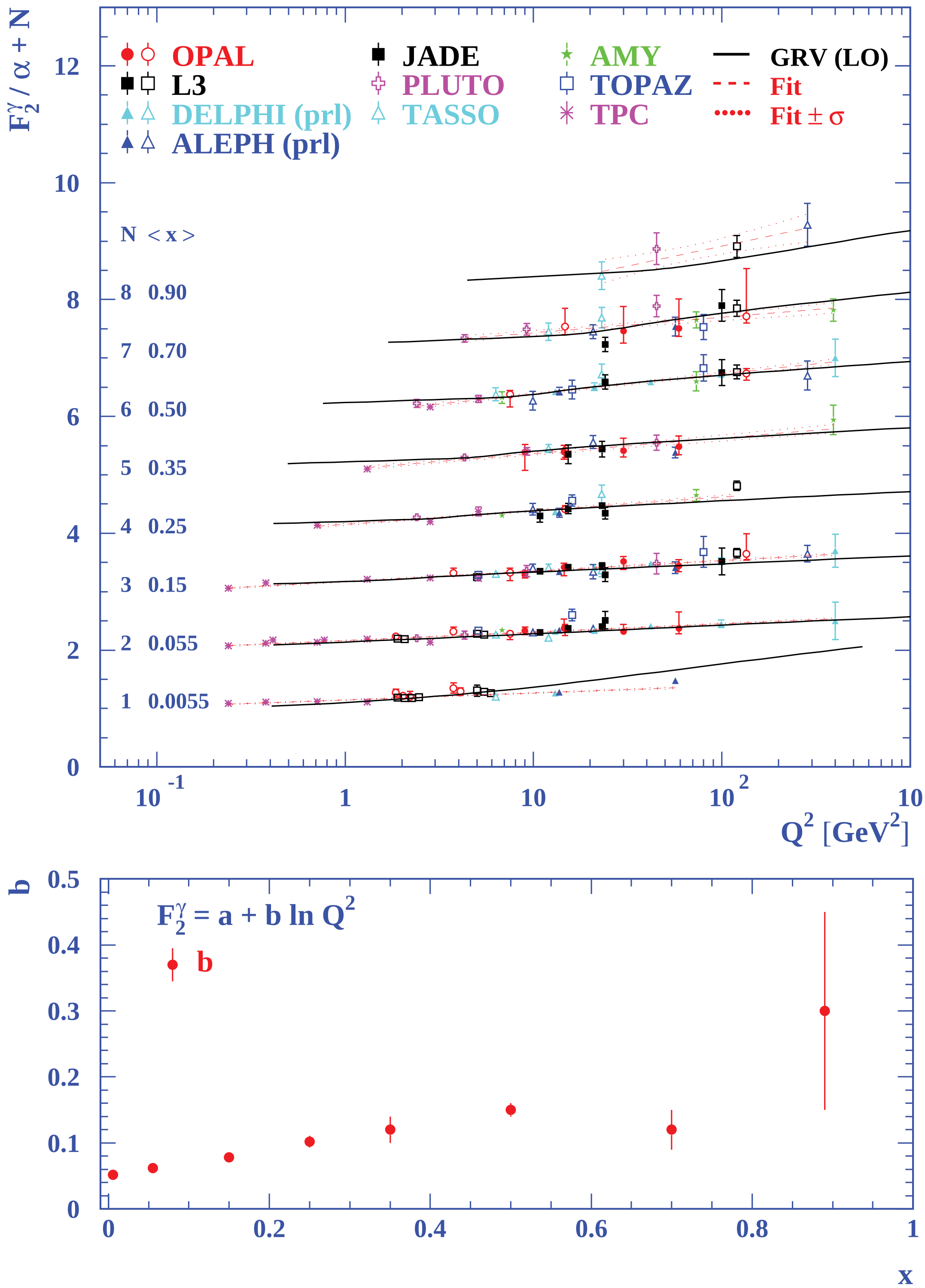

An increasing slope as a function of x is observed.

Q^2 evolution after charm subtraction

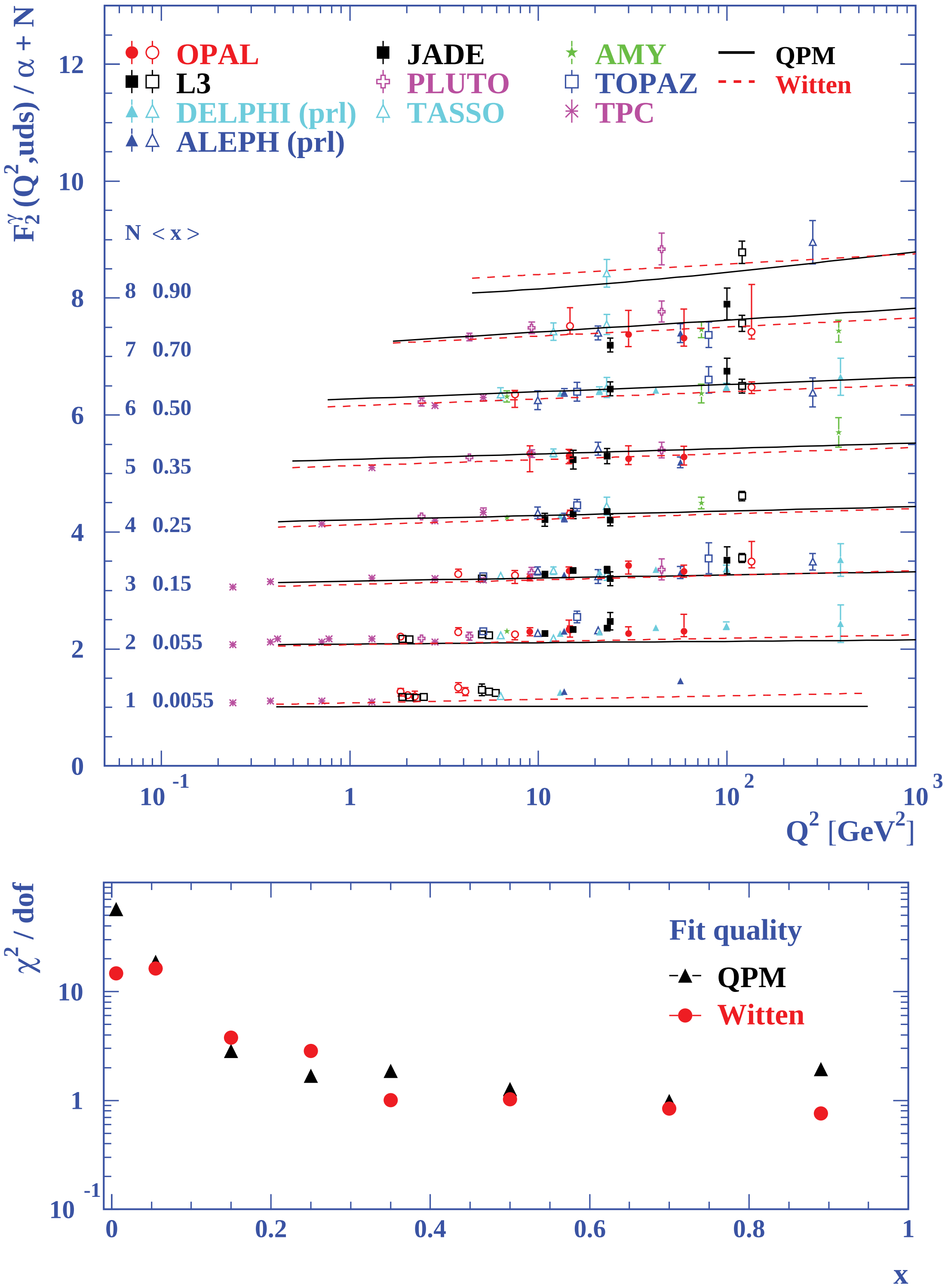

Which of the predictions are verified ?

QED structure

1. The rise of the QED structure for large x ist clearly seen.
2. The P^2 suppression of the QED structure function is verified.
3. There is an indirect evidence for the existence of the interference terms.

Hadronic structure

1. The Q^2 evolution of the photon structure shows a clear rise for all values of x.
2. The acceptance is not sufficient to see the predicted rise at low values of x.

P^2 suppression of F_2^γ

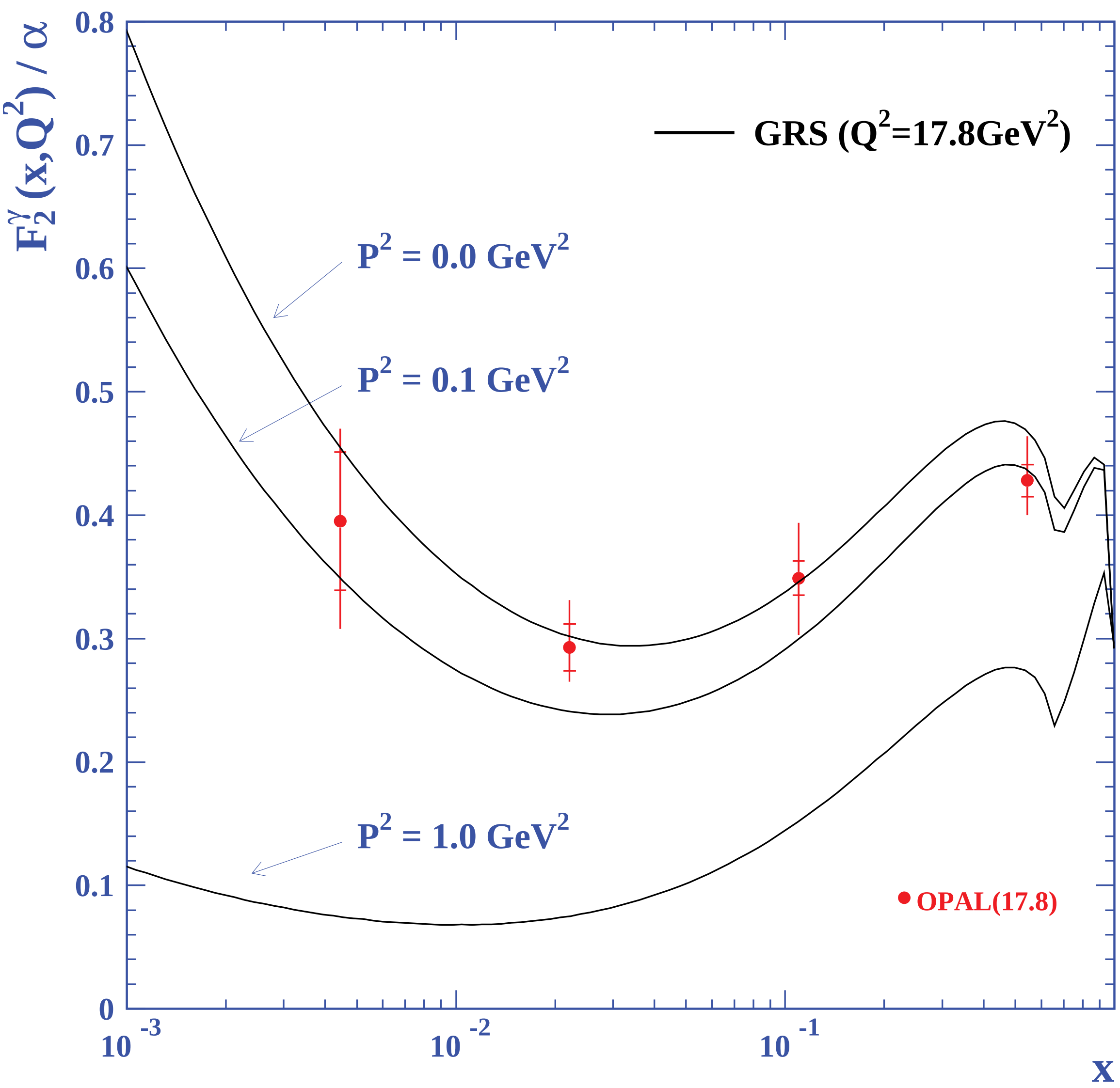

F_2^γ is suppressed by about 30-60% for virtualities of

$P^2 = 0.1\text{-}1.0\ \mathrm{GeV}^2$.

Good P^2 resolution ⇔ spatial resolution is needed.

The OPAL far-forward calorimeter

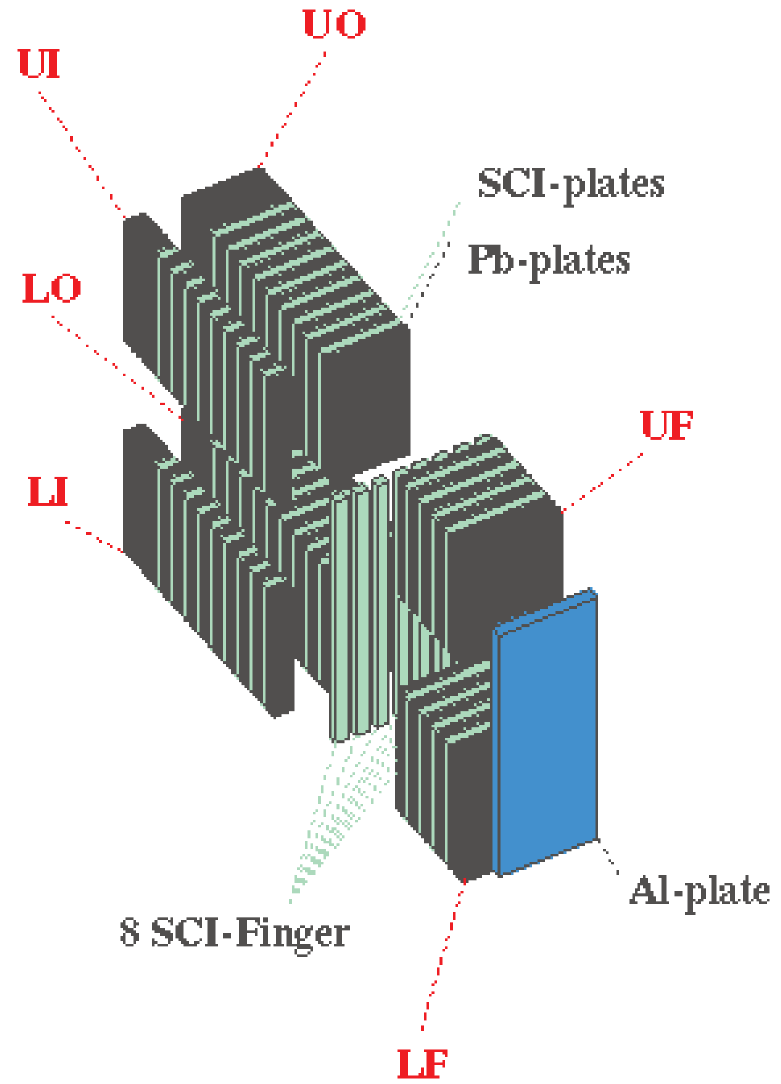

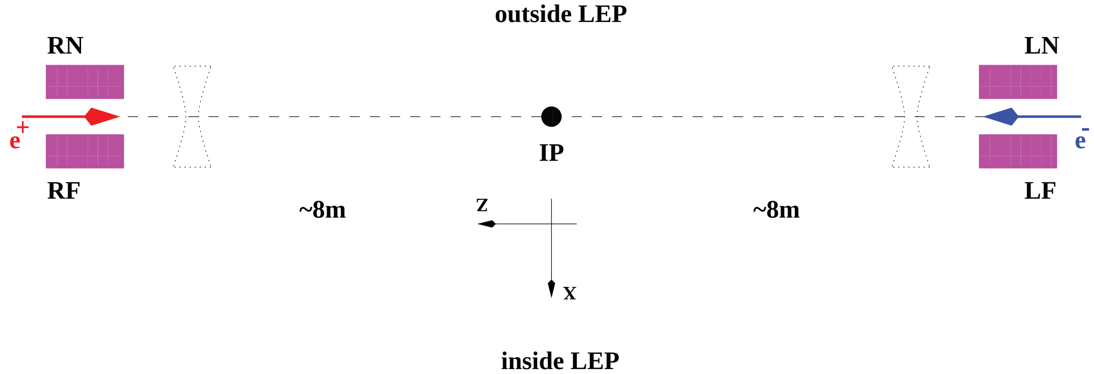

Data versus Monte Carlo for bhabha events

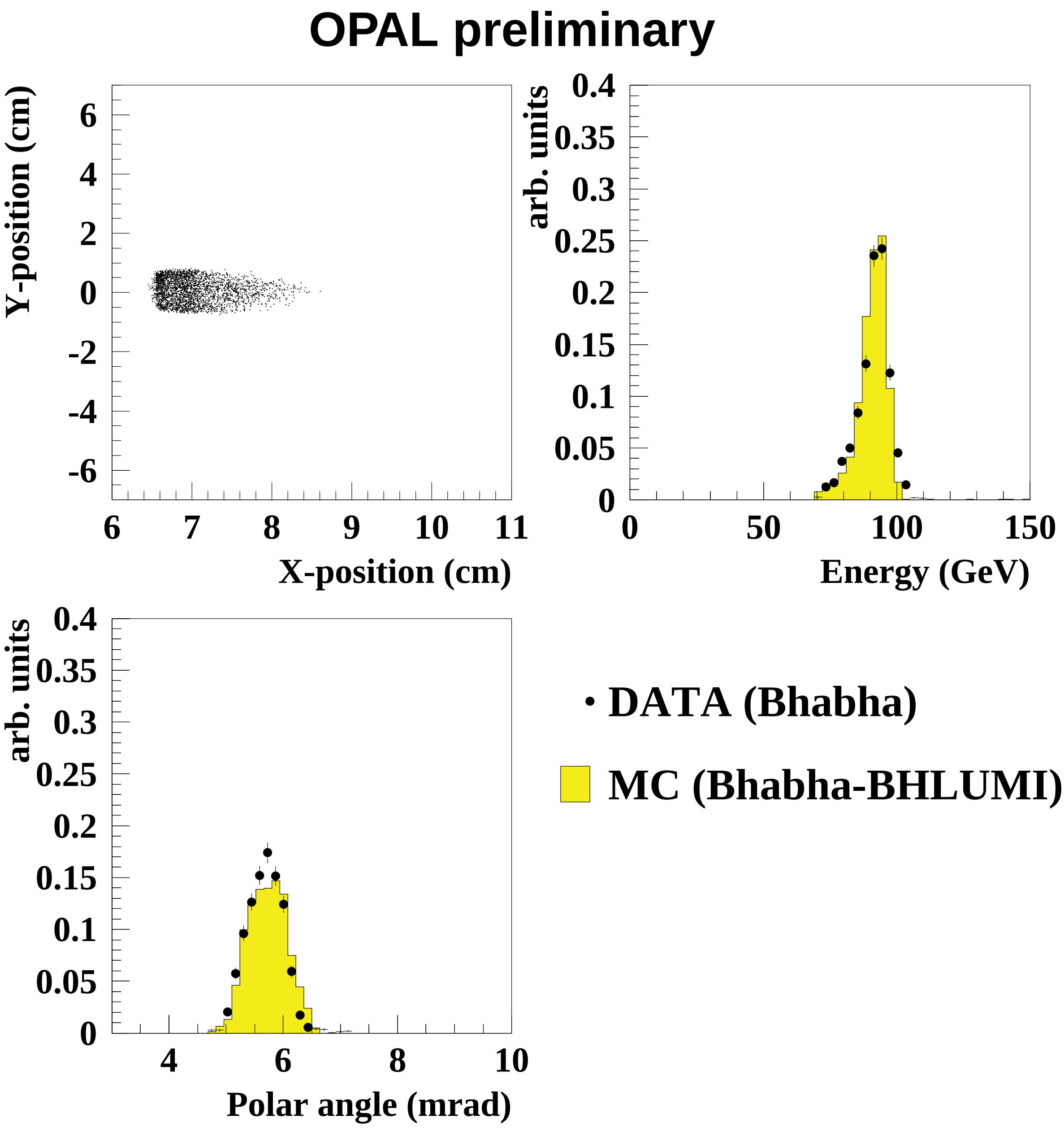

The detector behaviour is sufficiently well understood.

Leading order diagrams

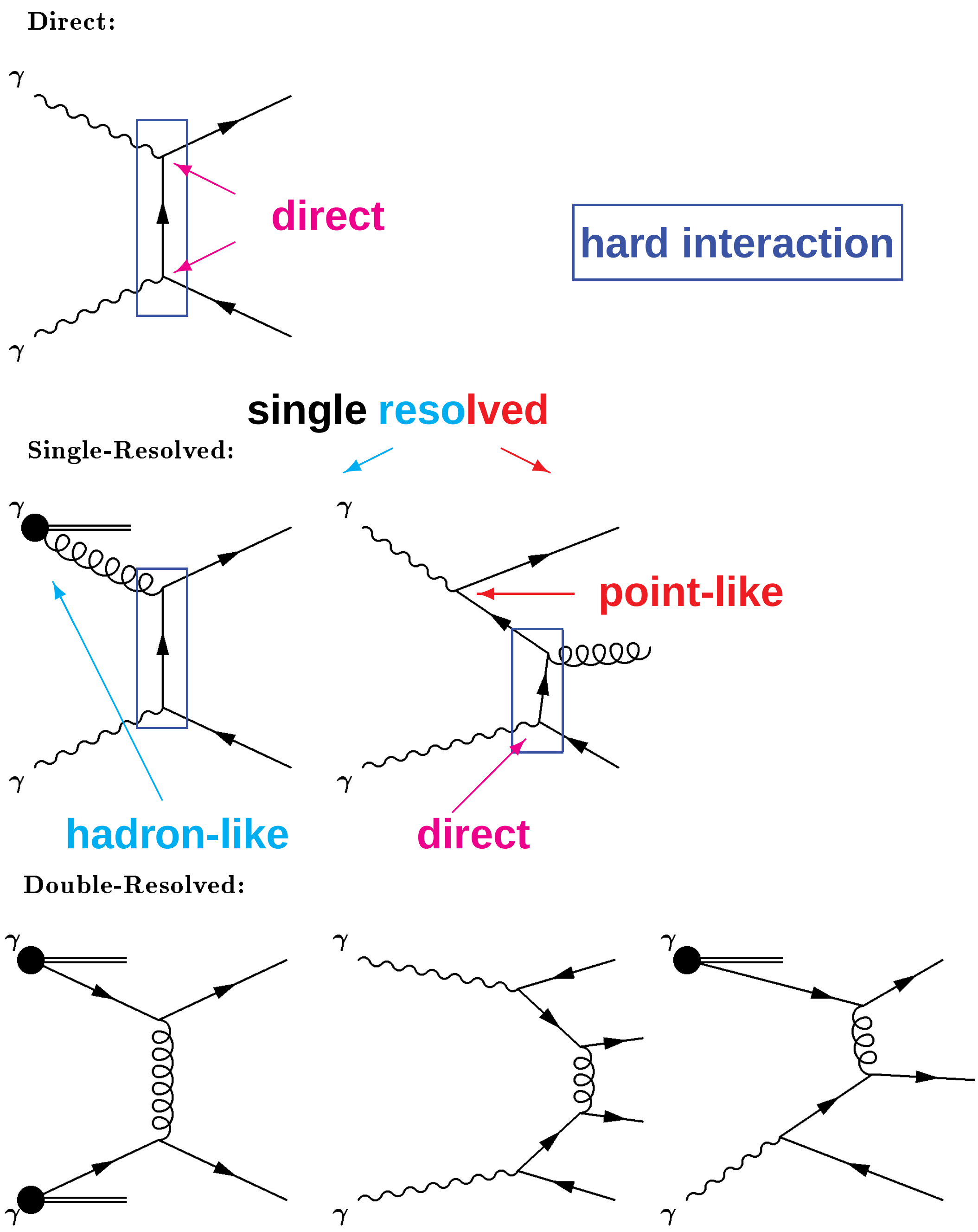

W distributions for anti-tagged events

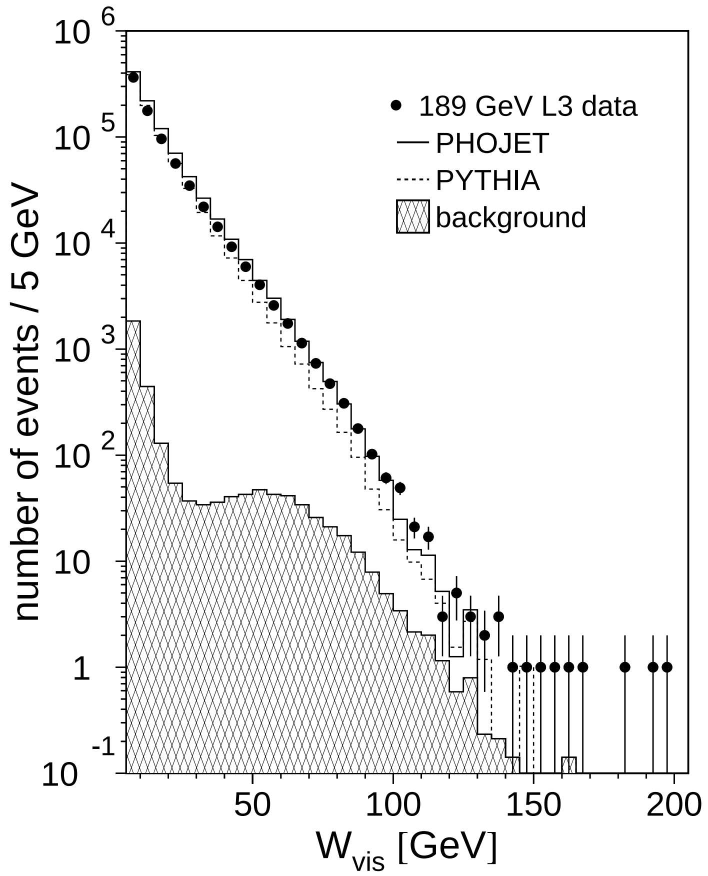

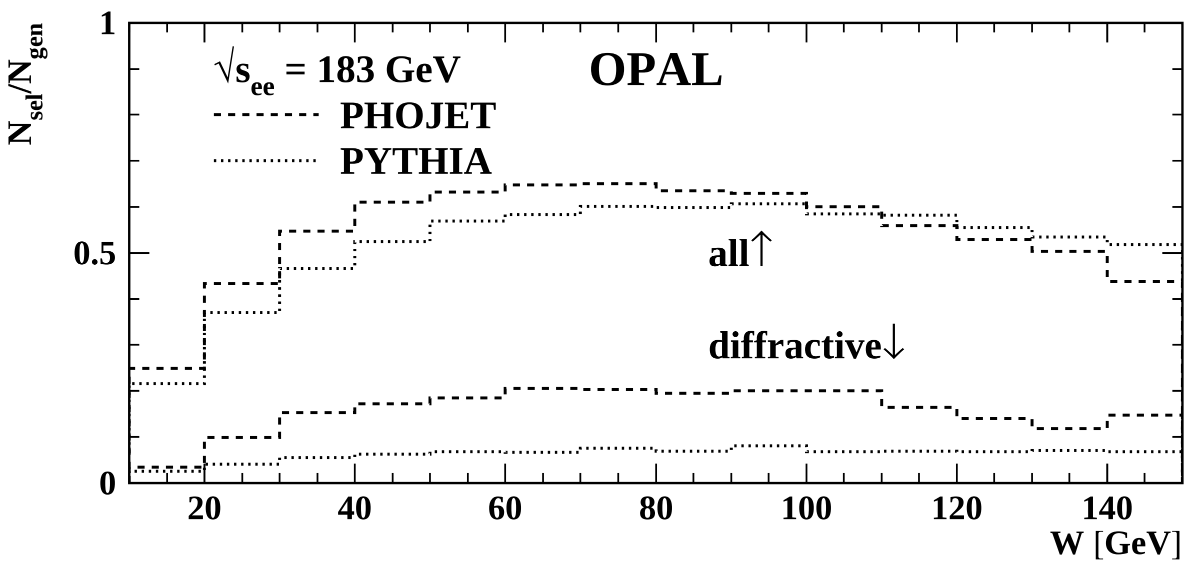

The acceptance for diffractive and elastic events is very different for the PHOJET and PYTHIA models

The total hadronic cross-section $\sigma_{\gamma\gamma}$

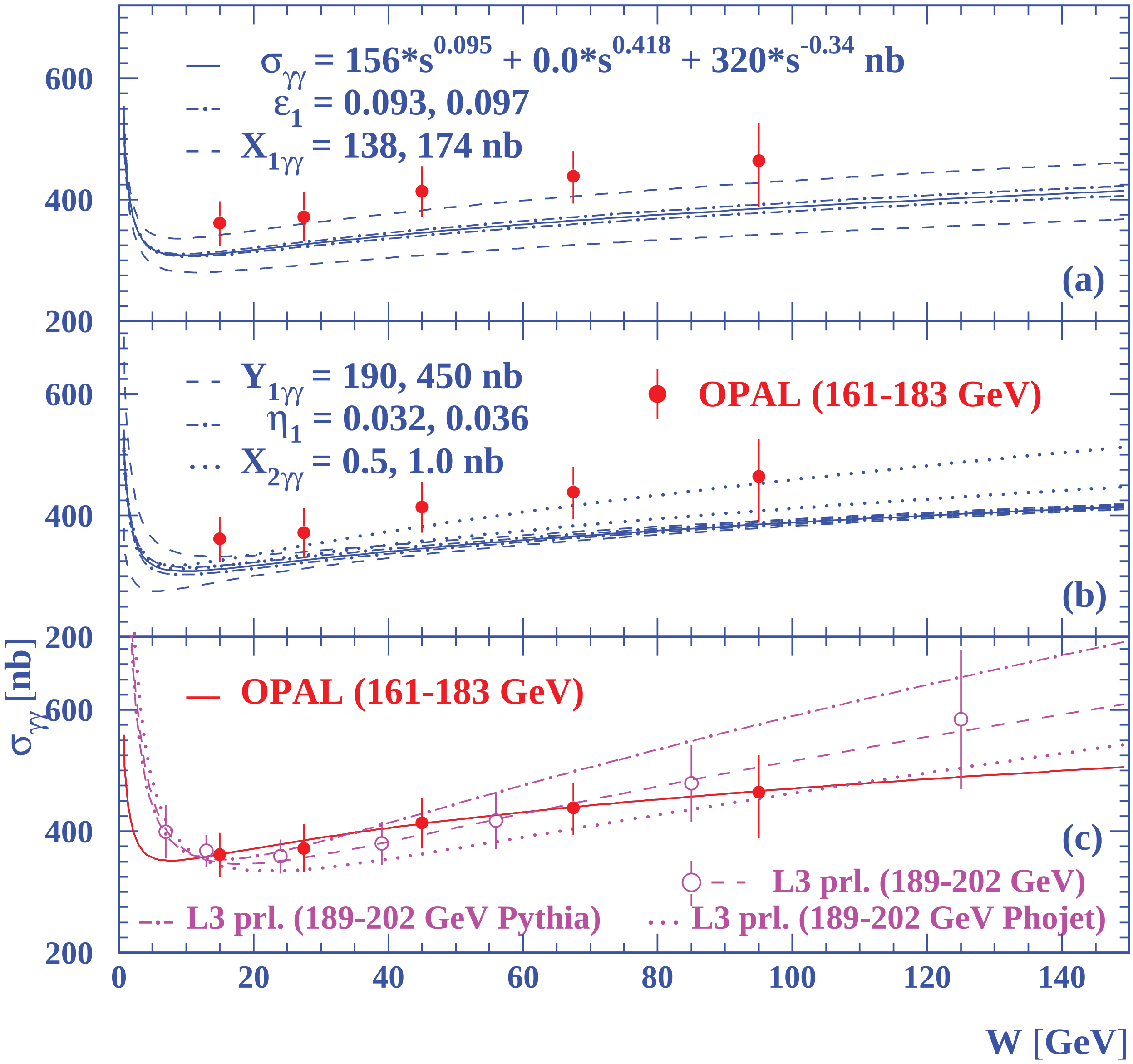

A clear rise of the total cross-section is observed in the data.

The concept of effective parton distribution functions

$$\frac{\mathrm{d}^5\sigma}{\mathrm{d}z\,\mathrm{d}x_\gamma\,\mathrm{d}x_\mathrm{p}\,\mathrm{d}\cos\theta^\star\,\mathrm{d}P^2} \propto \frac{1}{z}\frac{\mathrm{d}^2N_\gamma^\mathrm{T}}{\mathrm{d}z\,\mathrm{d}P^2}\frac{\tilde{f}_\gamma(x_\gamma,Q^2,P^2)}{x_\gamma}\frac{\tilde{f}_\mathrm{p}(x_\mathrm{p},Q^2)}{x_\mathrm{p}}|M_\mathrm{SES}(\cos\theta^\star)|^2$$

with:

$$\tilde{f}_\mathrm{p}(x_\mathrm{p},Q^2) \equiv \sum_{k=1}^{n_f}\left[\,q_k^\mathrm{p}(x_\mathrm{p},Q^2) + \bar{q}_k^\mathrm{p}(x_\mathrm{p},Q^2)\,\right] + \frac{9}{4}g^\mathrm{p}(x_\mathrm{p},Q^2)$$

$$\tilde{f}_\gamma(x_\gamma,Q^2,P^2) \equiv \sum_{k=1}^{n_f}\left[q_k^\gamma(x_\gamma,Q^2,P^2) + \bar{q}_k^\gamma(x_\gamma,Q^2,P^2)\right] + \frac{9}{4}g^\gamma(x_\gamma,Q^2,P^2)$$

$$\tilde{f}_\gamma = \tilde{f}_\gamma^\mathrm{T} + \frac{2(1-z)}{1+(1-z)^2}\tilde{f}_\gamma^\mathrm{L}$$

$$\frac{\mathrm{d}^2N_\gamma^\mathrm{T}}{\mathrm{d}z\,\mathrm{d}P^2} = \frac{\alpha}{2\pi}\left[\frac{1+(1-z)^2}{z}\frac{1}{P^2} - \frac{2\,m_\mathrm{e}^2\,z}{P^4}\right]$$

Structure of virtual photons from H1

Fractional momentum x

Factorisation scale

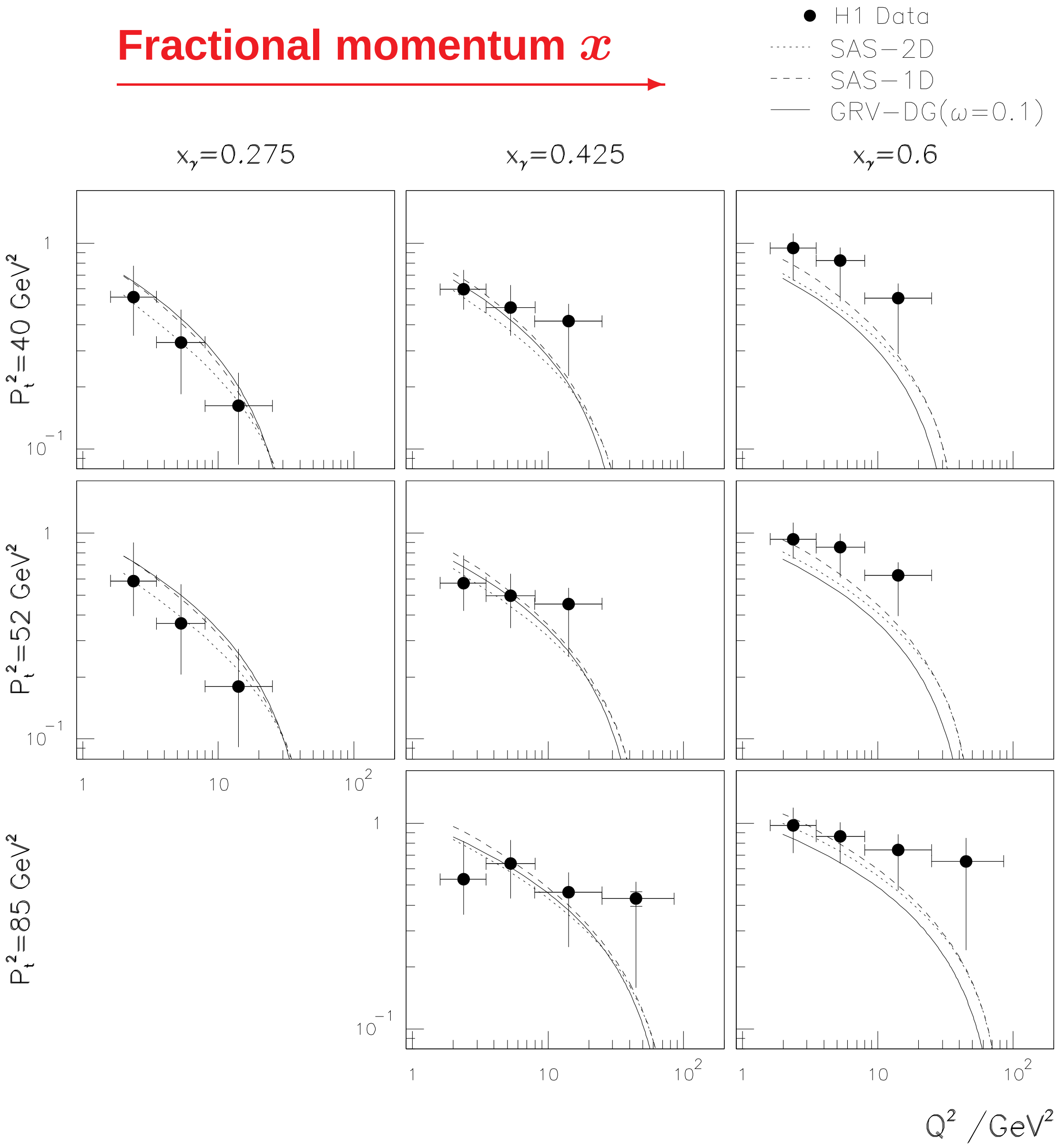

A strong suppression with increasing photon virtuality is observed.

Layout of a future Linear Collider

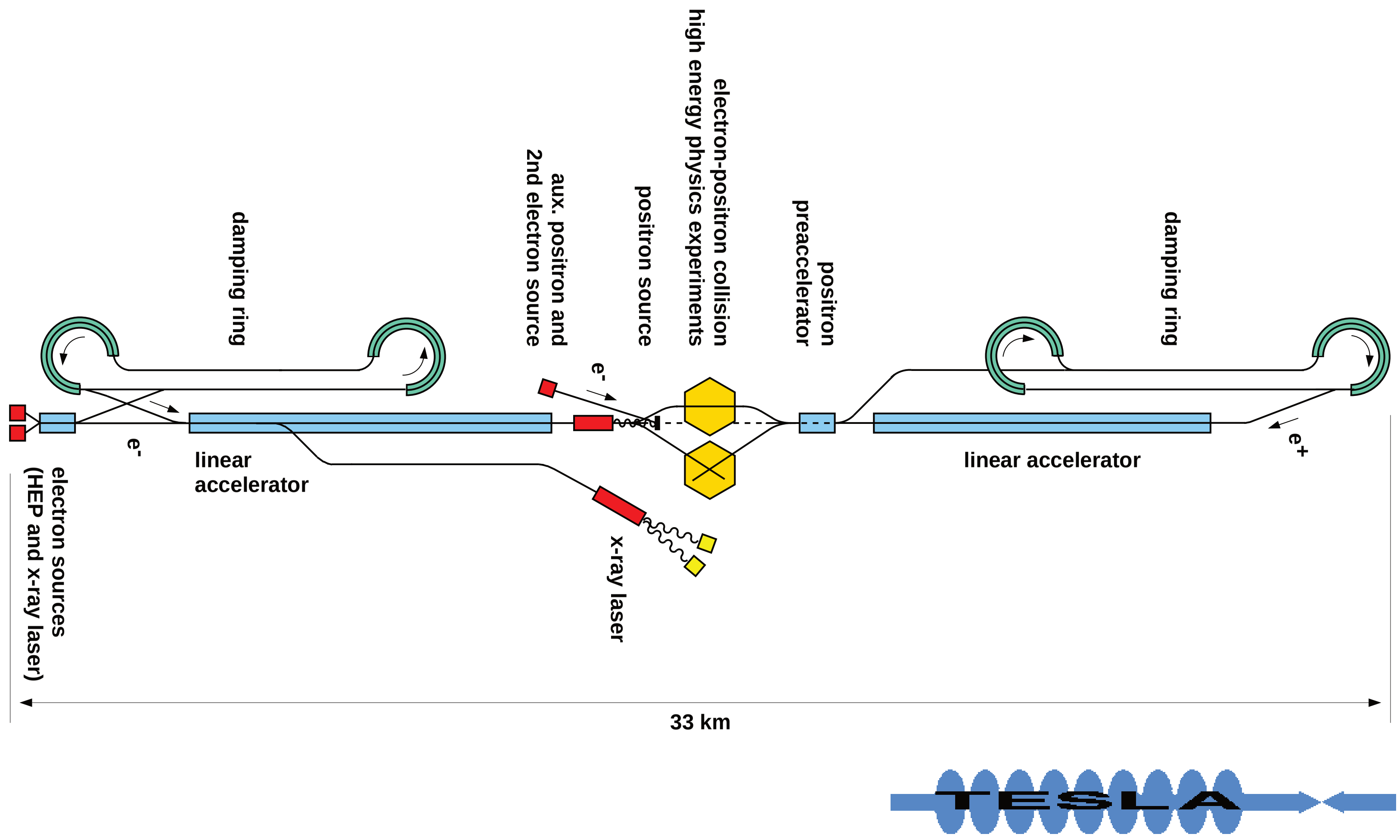

From LEP/ SLC to TESLA

LEP

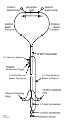

SLC

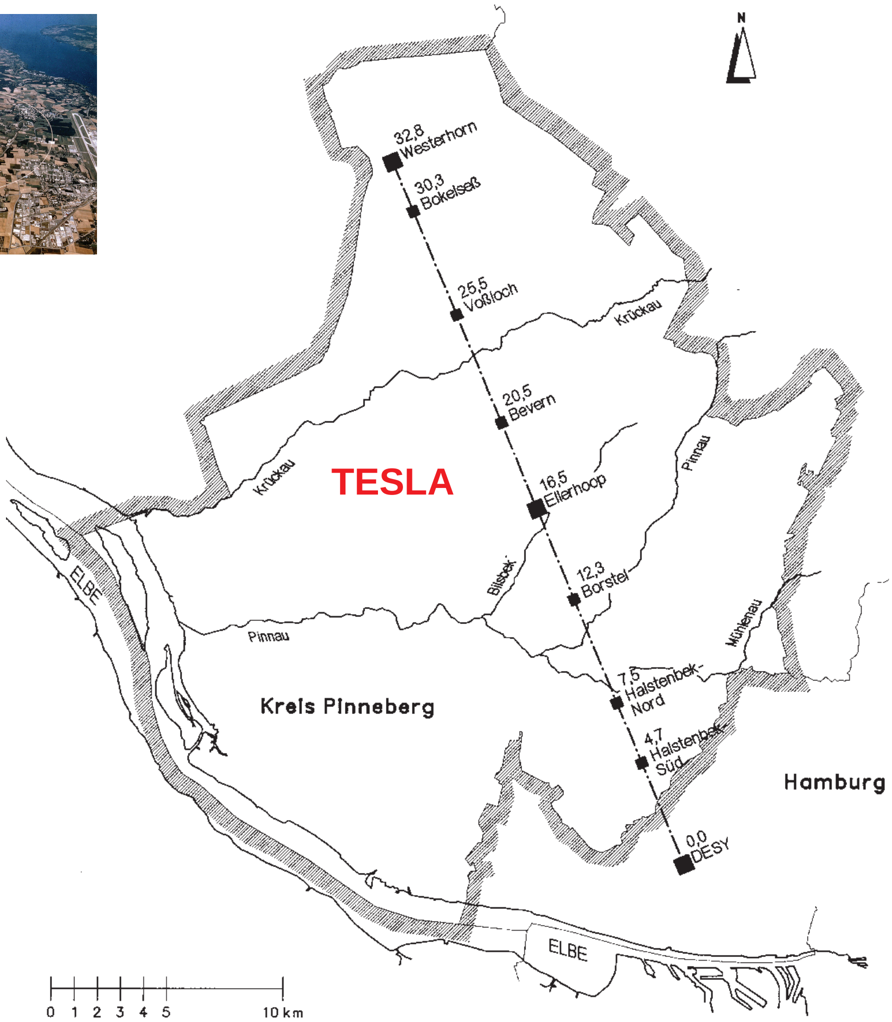

		LEP	SLC	TESLA
radius	[km]	8.5	∞	∞
length	[km]	26.7	4	33
gradient	[MV/m]	6	10	23,4
σ_x/σ_y	[μm/μm]	110 / 5	1.4 / 0.5	0.553/0.005
energy	[GeV]	100	50	250
lumi.	[10^{31}/cm^{2}s]	7.4	0.1	3400
$\mathcal{L}_{\rm int}$	[1/pb y]	250	15	10000

The future of the F_2^{γ} measurements

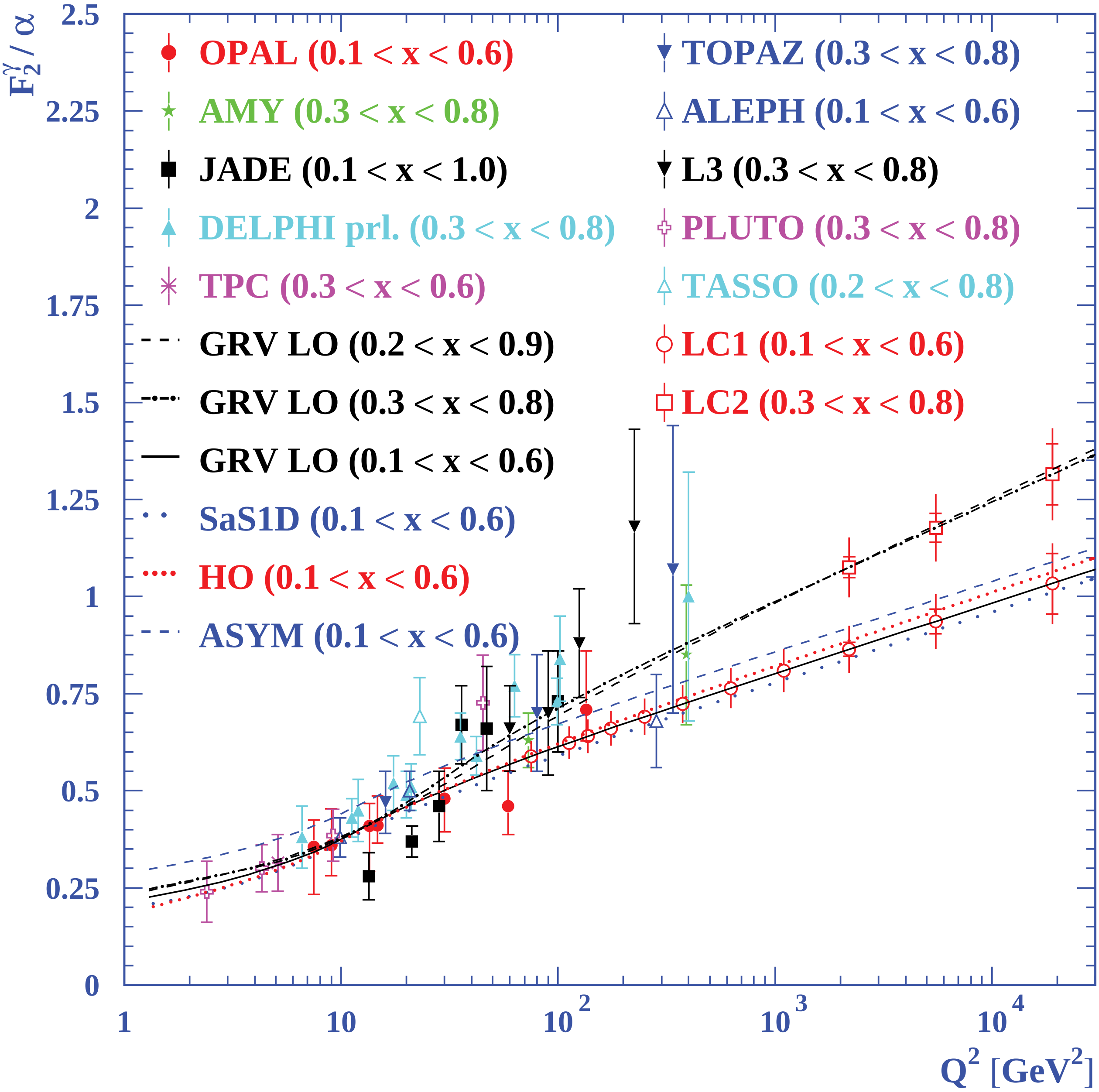

The Linear Collider (LC) will play an important role in testing this fundamental prediction of perturbative QCD.

Conclusion

- Many different measurements concerning the structure of the photon have been performed. The global properties of the photon are theoretically understood, however, there are many aspects which need improvements to arrive at a precise understanding of the structure of the photon.

Outlook

- With the large luminosity of the LEP program, and the improved understanding of the underlying physics, several measurements will get more precise.
- In the far future, the planned linear collider program will allow for an extension of the measurements of the photon structure to much larger momentum transfers.